

Journal Pre-proofs

Structure-activity relationships reveal a 2-furoyloxychalcone as a potent cytotoxic and apoptosis inducer for human U-937 and HL-60 leukaemia cells

Henoc del Rosario, Ester Saavedra, Ignacio Brouard, Daniel González-Santana, Celina García, Elena Spínola-Lasso, Carlos Tabraue, José Quintana, Francisco Estévez

PII: S0045-2068(22)00331-5
DOI: <https://doi.org/10.1016/j.bioorg.2022.105926>
Reference: YBIOO 105926

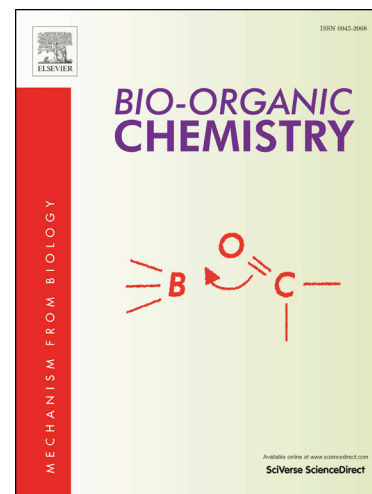
To appear in: *Bioorganic Chemistry*

Received Date: 7 March 2022
Revised Date: 25 May 2022
Accepted Date: 1 June 2022

Please cite this article as: H. del Rosario, E. Saavedra, I. Brouard, D. González-Santana, C. García, E. Spínola-Lasso, C. Tabraue, J. Quintana, F. Estévez, Structure-activity relationships reveal a 2-furoyloxychalcone as a potent cytotoxic and apoptosis inducer for human U-937 and HL-60 leukaemia cells, *Bioorganic Chemistry* (2022), doi: <https://doi.org/10.1016/j.bioorg.2022.105926>

This is a PDF file of an article that has undergone enhancements after acceptance, such as the addition of a cover page and metadata, and formatting for readability, but it is not yet the definitive version of record. This version will undergo additional copyediting, typesetting and review before it is published in its final form, but we are providing this version to give early visibility of the article. Please note that, during the production process, errors may be discovered which could affect the content, and all legal disclaimers that apply to the journal pertain.

© 2022 Published by Elsevier Inc.



Structure-activity relationships reveal a 2-furoyloxychalcone as a potent cytotoxic and apoptosis inducer for human U-937 and HL-60 leukaemia cells

Henoc del Rosario^a, Ester Saavedra^{a,b}, Ignacio Brouard^c, Daniel González-Santana^{c,d}, Celina García^e, Elena Spínola-Lasso^a, Carlos Tabraue^f, José Quintana^a, Francisco Estévez^{a,*}

^a Departamento de Bioquímica y Biología Molecular, Fisiología, Genética e Inmunología, Instituto Universitario de Investigaciones Biomédicas y Sanitarias (IUIBS), Grupo de Química Orgánica y Bioquímica, Universidad de Las Palmas de Gran Canaria, Unidad Asociada al Consejo Superior de Investigaciones Científicas (CSIC), 35016 Las Palmas de Gran Canaria, Spain

^b Instituto Canario de Investigación del Cáncer, 35016 Las Palmas de Gran Canaria, Spain

^c Instituto de Productos Naturales y Agrobiología, Consejo Superior de Investigaciones Científicas (IPNA-CSIC), 38206 La Laguna, Tenerife, Spain

^d Facultad de Farmacia. Universidad de La Laguna, Tenerife, Spain

^e Instituto Universitario de Bio-orgánica AG, Departamento de Química Orgánica, Universidad de La Laguna, Tenerife, Spain

^f Departamento de Morfología, Grupo de Investigación Medio Ambiente y Salud (GIMAS), Instituto Universitario de Investigaciones Biomédicas y Sanitarias (IUIBS), Universidad de Las Palmas de Gran Canaria, Las Palmas de Gran Canaria, Spain

*Corresponding author: francisco.estevez@ulpgc.es; Tel.: +34 928 451443

Abbreviations: CAT, catalase; DAPI, 4',6-diamidino-2-phenylindole; ERK, extracellular signal-regulated kinase; FMC, furoyloxymethoxychalcone; IC₅₀, 50% inhibition of cell growth; JNK/SAPK, *c-jun* N-terminal kinases / stress-activated protein kinases; MAPK, mitogen-activated protein kinases; MEK, mitogen-activated extracellular kinases; MTT, 3-(4,5-dimethyl-2-thiazolyl)-2,5-diphenyl-2H-tetrazolium bromide; PARP, poly(ADP-ribose) polymerase; p38^{MAPK}, p38 mitogen-activated protein kinases; ROS, reactive oxygen species.

Abstract

Synthetic flavonoids with new substitution patterns have attracted attention as potential anticancer drugs. Here, twelve chalcones were synthesized and their antiproliferative activities against five human tumour cells were evaluated. This series of chalcone derivatives was characterized by the presence of an additional aromatic or heterocyclic ring linked by an ether, in the case of a benzyl radical, or an ester or amide functional group in the case of a furoyl radical. In addition, the influence on cytotoxicity by the presence of one or three methoxy groups or a 2,4-dimethoxy-3-methyl system on the B ring of the chalcone scaffold was also explored. The results revealed that the most cytotoxic chalcones contain a furoyl substituent linked by an ester or an amide through the 2'-hydroxy or the 2'-amino group of the A ring of the chalcone skeleton, with IC₅₀ values between $0.2 \pm 0.1 \mu\text{M}$ and $1.3 \pm 0.1 \mu\text{M}$ against human leukaemia cells. The synthetic chalcone 2'-furoxyloxy-4-methoxychalcone (FMC) was, at least, ten-fold more potent than the antineoplastic agent etoposide against U-937 cells and displayed less cytotoxicity against human peripheral blood mononuclear cells. Treatment of U-937 and HL-60 cells with FMC induced cell cycle arrest at the G₂-M phase, an increase in the percentage of sub-G₁ and annexin-V positive cells, the release of mitochondrial cytochrome *c*, activation of caspase and poly(ADP-ribose) polymerase cleavage. In addition, it inhibited tubulin polymerization *in vitro* in a concentration dependent manner. Cell death triggered by this chalcone was decreased by the pan-caspase inhibitor z-VAD-fmk and was dependent of the generation of reactive oxygen species. We conclude that this furoxyloxychalcone may be useful in the development of a potential anti-leukaemia strategy.

Keywords: Apoptosis; Structure-activity relationship; Caspase; Cell cycle; Cytotoxicity; Chalcone, Furoxyloxychalcone

1. Introduction

Leukaemia is among the most commonly diagnosed cancers in adolescents and continues to be the leading cancer cause of death in the group aged 15 to 29 years [1]. In accordance with the GLOBOCAN database estimates of incidence and mortality worldwide for 2020, the estimated numbers of new cases and deaths from leukaemia were 474,519 and 311,594, respectively, emphasizing that mortality rates for this heterogeneous group of diseases are still very high [2], and requiring novel therapies to increase the efficacy.

Acute myeloid leukaemia is one of the most common leukaemias diagnosed in adults. The 5-year relative survival for children and adolescents is 67% but declines to 7% for patients aged 65 years and older [3]. Molecular targeted drugs and immunotherapies have improved the survival for hematopoietic and lymphoid malignancies but resistance to conventional therapies is one of the main limitations for treatment. The evasion of apoptosis is considered one of the mechanisms of resistance to conventional treatments against cancer. Apoptosis is a kind of regulated cell death, which results in targeted elimination of cells with minimal inflammatory response [4]. This cellular death is catalysed by the proteolytic activity of caspases, a family of cysteine-aspartate proteases which are expressed in cells as zymogens known as procaspases. These enzymes predominantly cleave their substrates on the C-terminal side of an aspartate residue [5]. Proteolytic cleavage leads to important biochemical and morphology changes such as phosphatidylserine exposure at the cell surface, plasma membrane blebbing, chromatin condensation, nuclear fragmentation and formation of apoptotic vesicles. Two main apoptotic pathways have been described, the intrinsic and the extrinsic pathways [6]. The intrinsic or mitochondrial pathway is initiated by perturbations of the intracellular or extracellular microenvironment, characterized by mitochondrial outer membrane permeabilization, cytosolic release of apoptogenic factors and caspase-3 activation. The extrinsic pathway is initiated from cell membrane proteins named as death receptors and characterized by caspase-8 activation and proteolytic maturation of executioner caspases, mainly caspase-3 [7].

Natural products represent realistic options as potential anticancer agents [8, 9]. Flavonoids are plant polyphenolic metabolites which exhibit remarkable pharmacological activities [10, 11].

These compounds are able to interfere in every phase of cancer progression by modulating key proteins involved in angiogenesis, apoptosis, differentiation, metastasis, proliferation and reverse multidrug resistance process [12]. In particular, the acyclic version of flavonoids, chalcones, are very simple small molecules with a privileged structure that exhibit relevant cytotoxicity against various cancer cells and low cytotoxicity against human normal cells [13,14]. Many natural products contain furan which is a relevant building block in the development of new therapies [15] and appears in 10 drugs approved by the FDA [16].

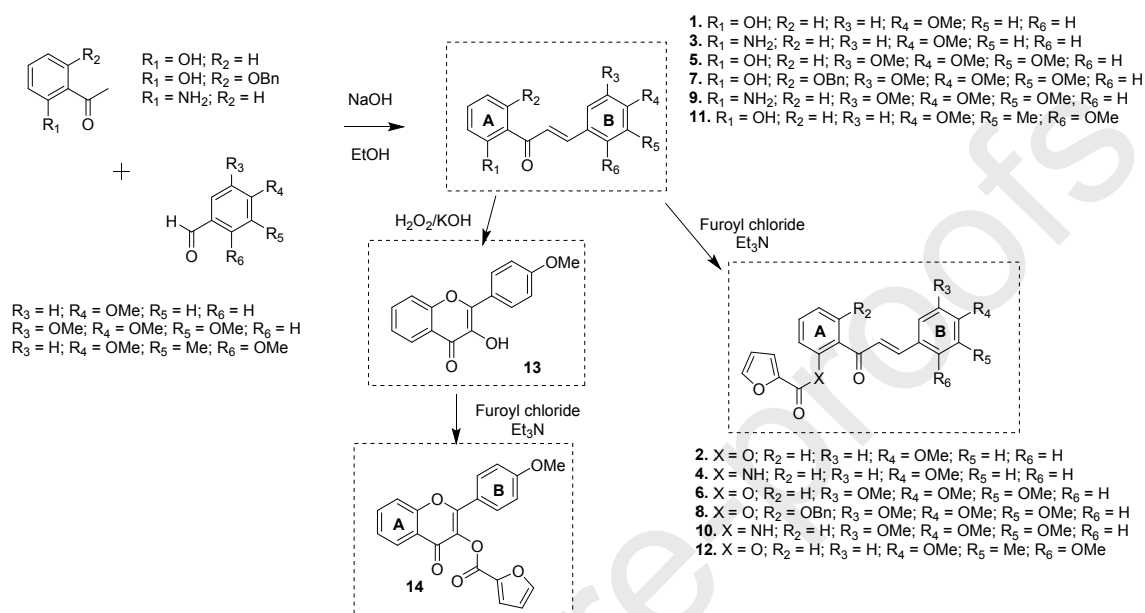
The aim of this study was (i) to synthesize a series of lineal chalcone derivatives together with two cyclic compounds containing electron donating groups (MeO- and Me-) on the B ring and (ii) to explore the effect of the presence of a furoyl substituent on the A ring of the chalcone skeleton on cytotoxicity against several human tumour cells. The basis for the design of these compounds is the application of the function-oriented synthesis (FOS) concept, a step-economic strategy directed to the synthesis of simple compounds with superior activity [17]. We have explored the influence of different substituents on both rings of the chalcone skeleton. These included (i) the presence of a hydroxyl group on the A ring or a benzyl radical, (ii) a furan ring linked by an ester or amide bond and (iii) the presence of a 4-methoxy or 3,4,5-trimethoxy or 2,4-dimethoxy-3-methyl systems on the B ring. In addition, we explored the signal transduction pathways of cell death triggered by 2'-furoyloxy-4-methoxychalcone, one of the most cytotoxic compounds against human U-937 and HL-60 leukaemia cells. These cell lines were selected as they are frequently used in biomedical research for the study of therapeutics and neoplasia and have made important contributions to the disciplines of immunology, hematology and cancer [18,19].

2. Results

2.1. Chemistry

In the present study, we explored the effects of a collection of 12 chalcones, a flavonol and a flavonol derivative on viability of human tumor cells. The chalcones (**1-12**) were prepared in a straightforward manner by a standard aldolic condensation procedure combining three different

acetophenones with three different benzaldehydes [20]. Additionally, flavonol derivative **14** was obtained through an esterification reaction from flavonol **13** which was synthesized by oxidative cyclization reaction of compound **1** (Scheme 1).



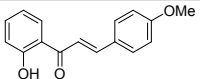
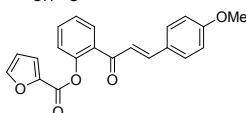
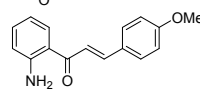
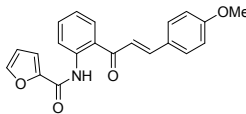
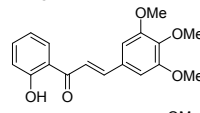
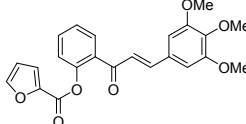
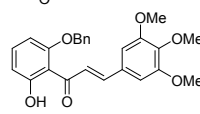
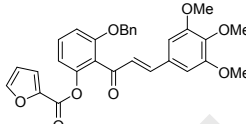
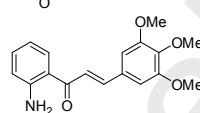
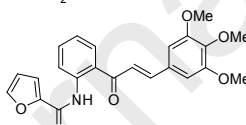
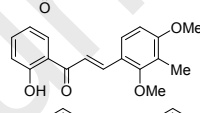
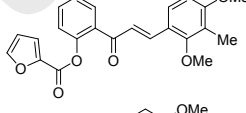
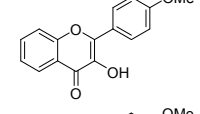
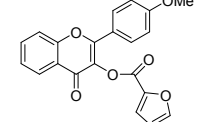
Scheme 1. Synthesis of chalcones and flavonols.

2.2. Biology

2.2.1. Screening of synthetic flavonoids reveals that 2'-furoyl-4-methoxychalcone inhibits the viability of human tumour cells

The SARs (structure-activity relationship) of a series of chalcones and two cyclic compounds were investigated for its potential cytotoxicity against human tumour cells. This series of compounds was characterized for the absence or the presence of a furoyl radical on the A ring and by a different substitution patterns on the B ring of the chalcone skeleton (Scheme 1). To this end, human tumour cells were treated with increasing concentrations of each compound and the IC_{50} values (the concentrations that induce a 50% inhibition of cell viability) were determined by the MTT assay (Table 1).

Table 1. Effects on cell viability of propenone derivatives on human tumour cells.

| Compound | IC ₅₀ (μM) | | | | |
|---|-----------------------|-------------|-------------|-------------|-------------|
| | U-937 | HL-60 | MOLT-3 | SK-MEL-1 | MEL-HO |
|  | 44.9 ± 4.4 | 35.2 ± 7.5 | 23.5 ± 9.9 | 40.7 ± 10.2 | 26.8 ± 2.1 |
|  | 0.2 ± 0.1 | 0.3 ± 0.1 | 0.6 ± 0.1 | 12.5 ± 1.5 | 2.0 ± 0.1 |
|  | 10.9 ± 2.4 | 12.4 ± 2.2 | 7.4 ± 1.1 | 28.2 ± 4.8 | 34.2 ± 7.9 |
|  | 0.9 ± 0.2 | 0.5 ± 0.2 | 1.3 ± 0.1 | 1.2 ± 0.6 | 11.8 ± 3.8 |
|  | 38.7 ± 8.5 | 46.6 ± 9.8 | 12.6 ± 5.8 | >100 | 71.1 ± 19.2 |
|  | 21.7 ± 12.3 | 23.1 ± 7.5 | 11.8 ± 6.7 | 30.3 ± 7.9 | 28.2 ± 2.7 |
|  | 4.1 ± 1.6 | 5.8 ± 2.2 | 3.6 ± 0.8 | 19.3 ± 2.4 | 11.9 ± 3.4 |
|  | 5.0 ± 1.6 | 3.6 ± 1.3 | 2.8 ± 0.5 | 17.8 ± 0.4 | 6.2 ± 1.6 |
|  | 5.9 ± 1.5 | 6.3 ± 0.9 | 6.4 ± 3.0 | 31.2 ± 3.1 | 11.6 ± 2.2 |
|  | 4.2 ± 1.5 | 26.1 ± 4.9 | 23.1 ± 8.6 | >100 | >100 |
|  | >100 | >100 | >100 | >100 | >100 |
|  | 7.1 ± 0.6 | 7.8 ± 1.8 | 5.8 ± 1.2 | >100 | >100 |
|  | 79.7 ± 21.6 | 55.9 ± 12.9 | 45.3 ± 10.2 | >100 | >100 |
|  | 50.4 ± 7.7 | 33.1 ± 12.4 | 5.6 ± 2.9 | >100 | 58.3 ± 26.6 |

Cells were incubated with increasing concentrations of the indicated compounds for 72 h and the IC₅₀ values were determined as described in the Material and methods Section. Data are expressed as means ± SEM from the dose-response curves of 3-5 independent experiments with three determinations in each.

Chalcone **1**, the first compound of this series, a 4-methoxy substituted chalcone exhibited low cytotoxicity against the human tumor cells assayed. However, the introduction of a furoyl radical as an ester at 2' position on the A ring in the chalcone skeleton enhanced the cytotoxicity approximately 200-fold in U-937 cells ($IC_{50} = 0.2 \pm 0.1 \mu\text{M}$ vs. $IC_{50} = 44.9 \pm 4.4 \mu\text{M}$ for chalcone **2** and chalcone **1**, respectively). This increase in cytotoxic activity was also observed in the other cell lines assayed. Cytotoxicity increased ~100-fold, 40-fold, 3-fold and 14-fold in HL-60, MOLT-3, SK-MEL-1 and MEL-HO, respectively. The substitution of the hydroxyl at 2' position of the A ring of chalcone **1** for an amino group to generate chalcone **3** increased ~4-fold the cytotoxicity against U-937 and ~3-fold against HL-60 and MOLT-3 cells. However, this enhancement in cytotoxicity was not observed in MEL-HO melanoma cells.

The amidation of the amino group with furoyl chloride to afford chalcone **4** resulted in an amplification of cytotoxicity. The IC_{50} values were ~1 μM in leukaemia cells and also in SK-MEL-1. This structural modification displayed distinct cytotoxicity against melanoma cells. The amide chalcone **4** was almost 10-fold more cytotoxic than the corresponding ester **2** against SK-MEL-1 cells but not against MEL-HO cells.

The insertion of two additional methoxy groups in chalcone **1** setting up a 3,4,5-trimethoxy system on the B ring to furnish chalcone **5** did not affect the cytotoxicity against the leukaemia cells assayed, showing similar IC_{50} values. In contrast, this modification blocked totally the cytotoxicity against melanoma cells.

The introduction of a furoyl ester in chalcone **5** to generate chalcone **6** increased slightly the cytotoxicity in all cell lines assayed, except for MOLT-3 cells in which the IC_{50} values for **5** and **6** were similar. However, chalcone **6** was much less potent than chalcone **2**. In comparison to chalcone **2**, the results suggest that the insertion of two additional electron-donating methoxy groups at positions 3 and 5 on the B ring, led to an important reduction in the antiproliferative activity against leukaemia and melanoma cells. The presence of a benzyloxy group in 6' position on the A ring of chalcone **5** to generate chalcone **7** increased the cytotoxicity against U-937 and HL-60 cells by approximately 10-fold, with ~4-fold and ~6-fold increases against MOLT-3 and melanoma cells, respectively. However, the introduction of a furoyl radical in chalcone **7** to

generate chalcone **8** did not enhance the cytotoxicity, except for MEL-HO which increased 2-fold with respect to its precursor.

In the case of the 3,4,5-trimethoxychalcones, the substitution of the 2'-hydroxy in the ring A of compound **5** for an amino group, to generate amino-chalcone **9**, increased approximately 7-fold the cytotoxicity against U-937, HL-60 and MEL-HO cells. However, the introduction of a furoyl radical in the amino group (compound **10**) had different effects depending on the cell line. The IC_{50} values were similar for **9** and **10** in U-937 cells and there was a decrease in cytotoxicity against HL-60, MOLT-3 and melanoma cells.

Table 1 also provides important information regarding the presence of the furoyl radical on the A ring in the chalcone **11** containing a 2,4-dimethoxy-3-methyl substitution pattern on the B ring. Although compound **11** did not display cytotoxicity against cancer cells ($IC_{50} > 100 \mu\text{M}$), the esterification of the hydroxy group at 2' position of the A ring with 2-furoyl chloride led to an increase in cytotoxicity in the three leukaemia cells assayed (IC_{50} values of $7.1 \pm 0.6 \mu\text{M}$, $7.8 \pm 1.8 \mu\text{M}$ and $5.8 \pm 1.2 \mu\text{M}$ for compound **12** in U-937, HL-60 and MOLT-3, respectively). However, this modification did not affect the cytotoxicity against SK-MEL-1 and MEL-HO melanoma cells.

The effect of the cyclization of chalcone **1** to yield the flavonol **13** and its furoyl ester derivative **14** on cytotoxicity was also explored. In general, a great reduction in the cytotoxicity was observed except for compound **14** in leukaemia cells (Table 1). The SAR of chalcones derivatives are displayed graphically in Figure 1. The most relevant results are that the cytotoxicity improved by (i) the presence of a furoyl radical as an ester or an amide, (ii) the substitution of the 2'-hydroxyl for an amino group at least against human leukaemia cells, and (iii) the presence of a benzyloxy group. However, cyclization led to a major reduction in cytotoxicity.

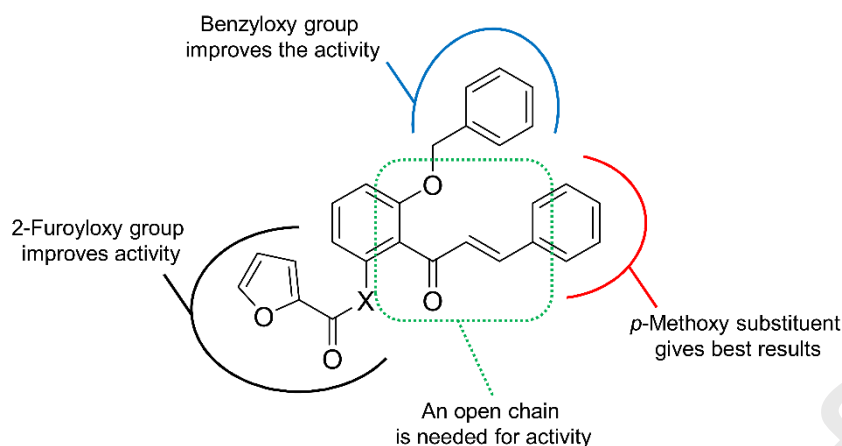


Figure 1. Structure-activity relationship of chalcone analogues.

These results suggest that the main determinant of cytotoxicity in 4-methoxy-chalcone is the presence of a furoyl radical on the A ring, and that one of the most cytotoxic compounds was the chalcone **2** in all cell lines assayed (Table 1). In these experiments, the antineoplastic agent etoposide was included as a positive control for U-937 ($IC_{50} = 1.4 \pm 0.3 \mu M$), HL-60 ($IC_{50} = 0.5 \pm 0.1 \mu M$) and MOLT-3 ($IC_{50} = 0.3 \pm 0.1 \mu M$).

Since the furoylchalcone **2** (FMC) was found to be one of the most cytotoxic compounds, it was selected for further experiments using the human histiocytic lymphoma U-937 and the human myeloid leukaemia HL-60 cells as models. In accordance with the concentration-dependent inhibition of viability, FMC induced significant morphological changes and caused an important decrease in the number of cells, as visualized by phase-contrast microscopy (Figure 2a and 2b). When U-937 and HL-60 cells were treated with FMC ($0.3 \mu M$) for 12 days the colony formation was almost completely inhibited as well as the volume of the colonies, in a similar way to the antitumor etoposide ($0.2 \mu M$) which was used as a positive control (Figure 2c). Human quiescent peripheral blood mononuclear cells obtained from healthy donors were more resistant to the effects on viability of FMC than U-937 and HL-60 cells. Although proliferating lymphocytes were more sensitive than quiescent mononuclear cells they were also slightly more resistant than leukaemia cells. In addition, the fibroblast-like Vero cells showed less cytotoxicity even at $10 \mu M$ FMC for 24 h. These results indicate that FMC inhibits the viability of leukaemia cells while

normal quiescent lymphocytes showed no appreciable toxicity up to 10 μM of chalcone for 24 h (Figure 2d).

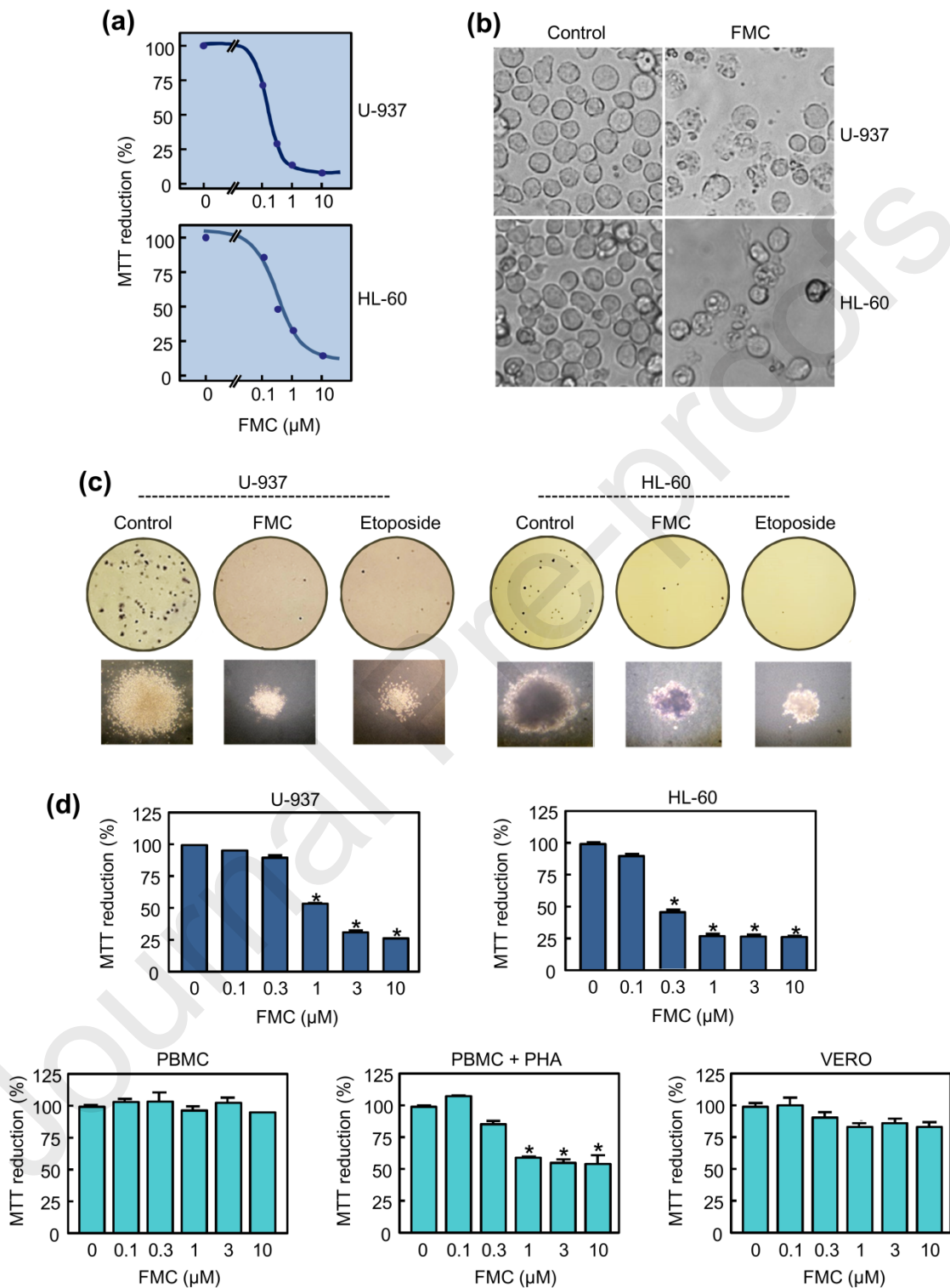


Figure 2. FMC inhibited viability of human U-937 and HL-60 cells. (a) Cells were cultured with increasing concentrations of FMC for 72 h and mitochondrial respiratory function was determined by the MTT assay. (b) Cells were treated with 3 μM FMC for 24 h and images were obtained with an inverted phase-contrast microscope; original magnification 20x. (c) Soft agar colony formation assay. Cells were plated in a soft agar colony formation assay with vehicle (DMSO), 0.3 μM FMC or 0.2 μM etoposide for twelve days and

the colony formation ability was analyzed. Representative plates and colonies visualized by phase-contrast microscopy are shown. Picture of wells are representative of three independent experiments. (d) Differential effect of FMC on cell viability of human U-937 and HL-60 leukaemia cells vs. normal peripheral blood mononuclear cells (PBMC), phytohemagglutinine (PHA)-activated healthy human PBMC and Vero. Cells were cultured in the presence of the indicated concentrations of FMC for 24 h and mitochondrial respiratory function was determined by the MTT assay. Values represent means \pm S.E. of three independent experiments each performed in triplicate. * $P < 0.05$, significantly different from the untreated control.

2.2.2. *Furoyloxychalcone induced G₂-M arrest and apoptosis in human myeloid leukaemia cells*

To investigate whether the decrease in viability induced by FMC was caused by changes in cell cycle phases, flow cytometric analyses were included in this study. To this end, U-937 and HL-60 cells were incubated with increasing concentrations of FMC for different periods of time (6-24 h), stained with propidium iodide and analyzed by flow cytometry. As shown in Table 2 and Figure 3a, a concentration as low as 1 μ M was able to induce a G₂-M arrest after 6 h of treatment in both cell lines. The percentage of U-937 control cells in G₂-M phase was approximately 20%, which increased to 31%, 38% and 35% after treatment with 1 μ M, 3 μ M and 10 μ M FMC, respectively, and this was accompanied by a reduction in cells in the G₁ phase. The increase in G₂-M phase cell population was also observed at 12 h of treatment and this effect started diminishing at 24 h. In U-937 cells, the percentage of sub-G₁ (i.e., apoptotic cells) increased until 14.3% (~4-fold), 20.2% (10-fold) and 53.3% (23-fold) by 3 μ M FMC after 6, 12 and 24 h of treatment, respectively. Similar results were obtained in HL-60 cells. The percentage of HL-60 cells in G₂-M was ~20% which increased to 33% and 43% after 6 h and 12 h of treatment with 3 μ M FMC, respectively. This G₂-M arrest decreased after 24 h of treatment and was associated with a fifty-fold increase in the percentage of sub-G₁ cells (1.1% vs. 54.8%). Representative histograms of flow cytometry after propidium iodide labeling are shown in Figure 3a. Since FMC caused G₂-M phase arrest, whether this chalcone might affect tubulin polymerization was investigated using an *in vitro* assay and monitoring the increase in absorbance of the reaction mixture. The results demonstrated that FMC inhibited tubulin polymerization in a concentration-dependent manner. In these experiments colchicine (5 μ M) and taxol (10 μ M) were used as positive controls of inhibition and promotion of tubulin polymerization, respectively (Figure 3b). The IC₅₀ value for inhibition of tubulin polymerization (defined as the compound concentration that inhibited the extent of assembly by 50% after 20 min incubation at 37 °C) was $4.9 \pm 1.3 \mu$ M

(mean \pm S.E.; n = 3). To prove that FMC interferes with the microtubule network we performed immunofluorescence techniques using a monoclonal α -tubulin antibody. As shown in Figure 3c, visualized by fluorescence microscopy, FMC treatment disrupted the tubulin network in a similar way to colchicine (0.1 μ M). As expected, taxol (0.2 μ M) enhanced microtubule polymerization with an increase in the density of cellular microtubules. These results indicate that FMC inhibited the polymerization of microtubules in leukaemia cells.

To explore whether the molecular mechanism of FMC-induced G₂-M cell cycle arrest in leukaemia cells involves up-regulation of the cyclin-dependent kinase inhibitor p21^{Cip1/WAF1}, time-course and dose-response experiments were performed and p21^{Cip1/WAF1} levels were determined by Western blot. As shown in Figure 4a, FMC caused a time- and concentration-dependent up-regulation of p21^{Cip1/WAF1} in both cell lines. The quantification of apoptosis obtained by measurement of the number of sub-G₁ cells by flow cytometry reveals that maximum levels of apoptosis induction were obtained after treatment with 3 μ M FMC for 24 h in both cell lines (Table 2, Figure 4b).

Table 2. Effects of FMC on cell cycle phase distribution of human leukaemia cells.

| | | FMC (μM) | %Sub-G ₁ | %G ₁ | %S | %G ₂ -M |
|-------|------|-----------------------|---------------------|-----------------|-----------------|--------------------|
| U-937 | 6 h | 0 | 3.8 \pm 1.1 | 51.9 \pm 1.6 | 24.2 \pm 2.1 | 19.9 \pm 0.7 |
| | | 1 | 15.7 \pm 0.3 | 26.0 \pm 0.8* | 26.6 \pm 0.3 | 31.2 \pm 0.3* |
| | | 3 | 14.3 \pm 0.9* | 19.0 \pm 1.5* | 27.7 \pm 0.6 | 38.2 \pm 2.5* |
| | | 10 | 13.6 \pm 1.1* | 20.6 \pm 0.6* | 29.4 \pm 0.3* | 35.4 \pm 0.8* |
| | 12 h | 0 | 2.1 \pm 0.4 | 48.5 \pm 1.1 | 25.1 \pm 0.7 | 22.2 \pm 0.6 |
| | | 1 | 18.8 \pm 0.3* | 12.4 \pm 2.5* | 22.5 \pm 0.9 | 43.4 \pm 1.7* |
| | | 3 | 20.2 \pm 1.6* | 7.7 \pm 0.7* | 24.7 \pm 1.2 | 44.4 \pm 1.1* |
| | | 10 | 17.2 \pm 0.1* | 10.2 \pm 0.4* | 26.6 \pm 0.5 | 43.0 \pm 0.4* |
| | 24 h | 0 | 2.3 \pm 0.4 | 53.1 \pm 1.6 | 23.8 \pm 0.6 | 19.2 \pm 1.1 |
| | | 1 | 11.3 \pm 2.7* | 36.1 \pm 2.2* | 28.4 \pm 0.3* | 20.2 \pm 0.6 |
| | | 3 | 53.3 \pm 5.1* | 22.1 \pm 2.0* | 14.0 \pm 2.1* | 6.7 \pm 1.6* |
| | | 10 | 58.2 \pm 3.3* | 15.5 \pm 1.6* | 12.8 \pm 1.9* | 10.7 \pm 0.6* |
| HL-60 | 6 h | 0 | 2.9 \pm 0.7 | 44.3 \pm 0.0 | 31.2 \pm 0.2 | 21.5 \pm 0.4 |
| | | 1 | 7.1 \pm 0.9 | 24.3 \pm 0.1* | 35.3 \pm 0.2 | 33.0 \pm 0.8* |
| | | 3 | 7.2 \pm 1.4* | 22.4 \pm 0.5* | 36.3 \pm 1.8 | 33.9 \pm 0.0* |
| | | 10 | 6.3 \pm 0.4* | 24.3 \pm 2.3* | 35.6 \pm 0.6 | 33.4 \pm 2.0* |
| | 12 h | 0 | 2.6 \pm 0.2 | 48.3 \pm 0.5 | 29.3 \pm 0.5 | 19.2 \pm 0.4 |
| | | 1 | 11.2 \pm 1.5 | 18.6 \pm 2.8 | 31.6 \pm 0.9 | 37.4 \pm 0.7* |
| | | 3 | 13.2 \pm 1.0* | 8.5 \pm 0.4* | 33.5 \pm 1.6* | 43.8 \pm 0.2* |
| | | 10 | 11.6 \pm 3.0* | 9.9 \pm 0.4* | 32.6 \pm 0.2* | 45.1 \pm 3.6* |
| | 24 h | 0 | 1.1 \pm 0.2 | 52.7 \pm 0.2 | 30.2 \pm 0.7 | 15.7 \pm 0.7 |
| | | 1 | 16.6 \pm 3.3* | 50.7 \pm 1.3 | 21.5 \pm 1.1* | 10.8 \pm 0.9 |
| | | 3 | 54.8 \pm 0.9* | 17.8 \pm 2.1* | 10.2 \pm 0.8* | 16.4 \pm 2.0 |
| | | 10 | 59.4 \pm 1.6* | 14.7 \pm 0.1* | 9.3 \pm 0.1* | 15.9 \pm 1.6 |

Cells were incubated with the specified concentrations of FMC for increasing times and the cell cycle phase distribution was determined by flow cytometry. The values are means \pm S.E. of two independent experiments with three determinations in each. Asterisks indicate a significant difference ($P < 0.05$) compared with the corresponding controls.

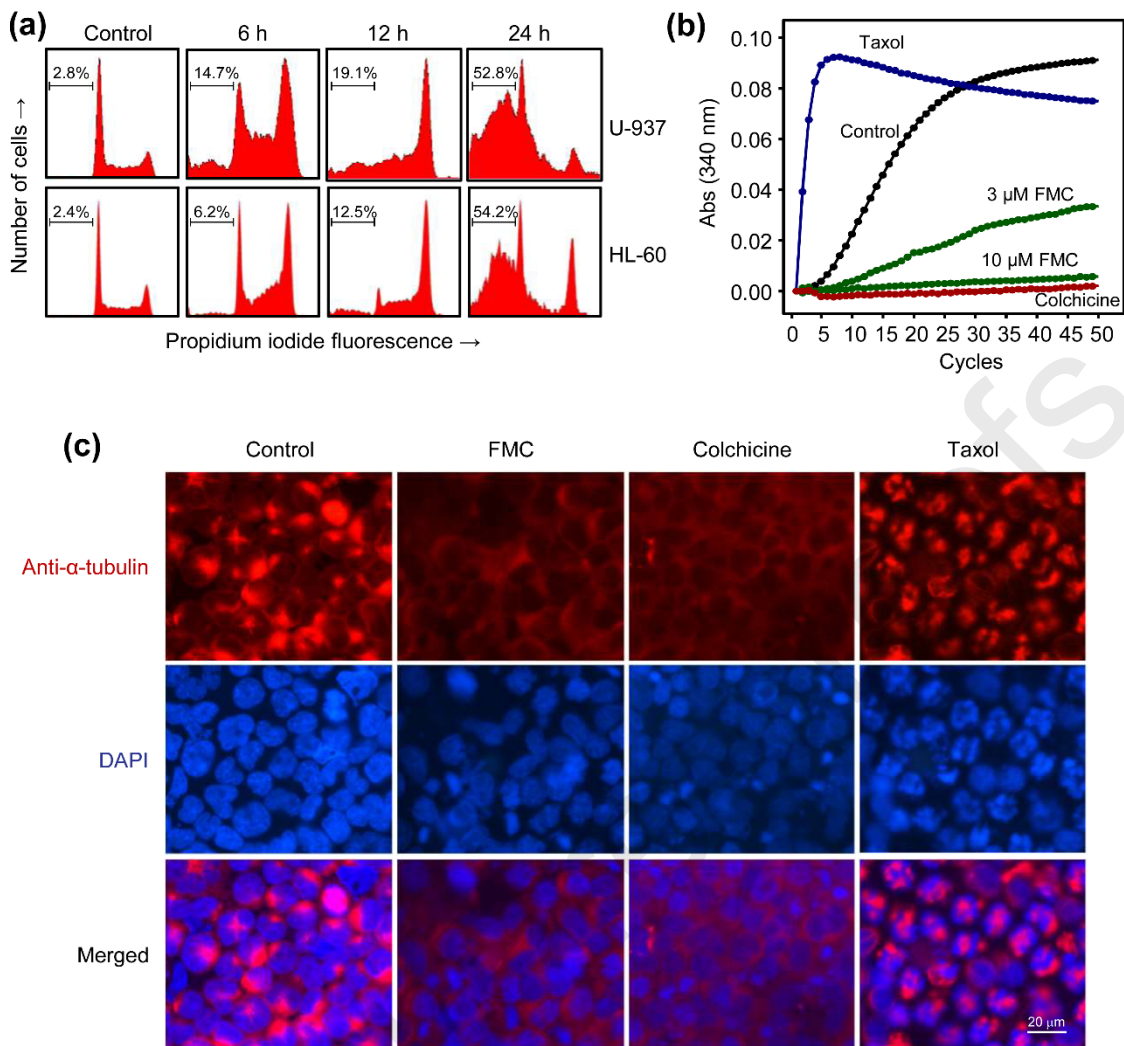


Figure 3. FMC induced cell cycle changes and inhibited the polymerization of microtubules. (a) Cells were cultured with 3 μM FMC for increasing periods of time, stained with propidium iodide and subjected to flow cytometry. Sub-G₁ cells (apoptotic cells) are shown in region marked with a bar. (b) FMC inhibited tubulin polymerization. Purified bovine brain tubulin was incubated at 37 °C in the absence (control) or in the presence of colchicine (5 μM), taxol (10 μM) or the specified concentrations of FMC and the absorbance at 340 nm was measured in a microplate reader. (c) Effect of FMC on the organization of cellular microtubule network. HL-60 cells were incubated with 3 μM FMC for 12 hours, harvested and fixed. Cells were then incubated with a monoclonal anti- α -tubulin antibody and after with an Alexa Fluor 594-conjugated secondary antibody. The cellular network of microtubules was analyzed using a Nikon fluorescent microscope. Colchicine (0.1 μM) and taxol (0.2 μM) were used as microtubule-depolymerization and -polymerization positive controls, respectively. Nuclear staining was performed with 1.5 $\mu\text{g}/\text{mL}$ DAPI (4',6-diamidino-2-phenylindole). Original magnification: 40x.

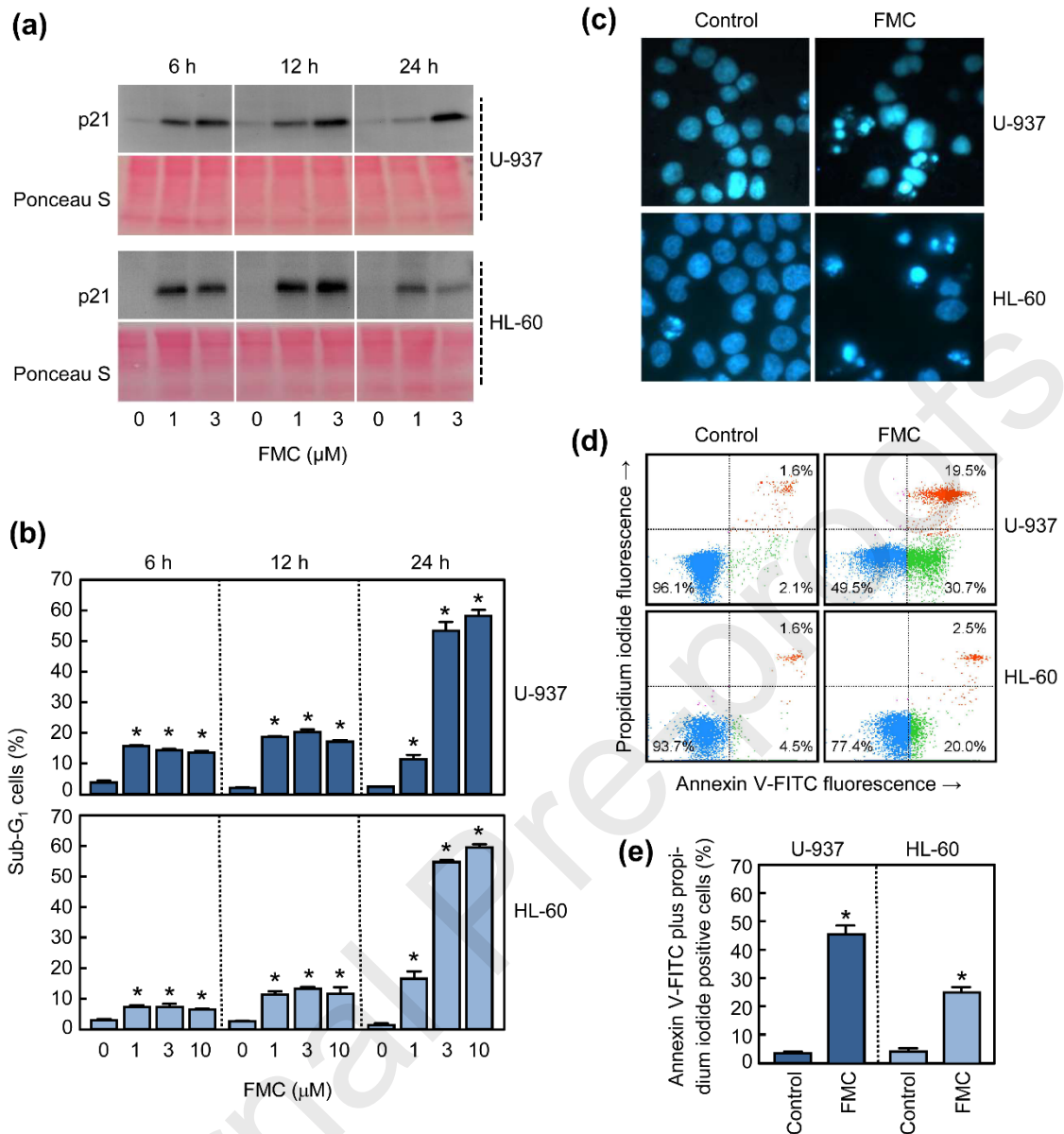


Figure 4. FMC induced apoptosis in human U-937 and HL-60 cells. (a) Cells were cultured with the indicated concentrations of FMC for the specified times and nuclear lysates were assayed by immunoblotting. Ponceau S staining was used as a transfer and loading control. A representative section is shown. (b) Cells were treated as indicated in (a) and apoptosis was quantified as percentage of sub-G₁ cells by flow cytometry. Values represent means \pm SEs of two independent experiments each performed in triplicate. * $P < 0.05$, significantly different from the untreated control. (c) Photomicrographs of representative fields of cells treated with 3 μ M FMC for 24 h and stained with Hoechst 33258. (d) Cells were treated as in (c), double stained with Annexin V-FITC and propidium iodide and subjected to flow cytometric analysis. (e) Cells were treated as in (d) and quantified by flow cytometry. Bars represent means \pm SEs of three independent experiments performed in duplicate. * $P < 0.05$, significantly different from the untreated control.

The nuclei of treated cells (3 μ M FMC, 24 h) visualized by fluorescence microscopy after Hoechst 33258 staining revealed condensation and fragmentation of chromatin (Figure 4c). In addition, the percentage of apoptotic cells, determined by the flow cytometric evaluation of the number of

annexin V-FITC positive cells (Figure 4d), increased fifteen times in U-937 cells treated with 3 μ M FMC for 24 h, and 4-fold in HL-60 cells (Figure 4e). These results indicate that FMC induces G₂-M phase arrest and apoptosis in human myeloid leukaemia U-937 and HL-60 cells.

2.2.3. *Furoxyloxychalcone induced caspase activation and poly(ADP-ribose) polymerase cleavage*

To explore whether the mechanism of cell death triggered by FMC in human leukaemia cells was associated with caspase activation, the enzymatic activity of cell lysates on specific tetrapeptide substrates was analyzed after treatment with 3 μ M FMC for different time periods. As shown in Figure 5a, maximal caspase-3/7, -8 and -9 activities were obtained after 24 h of treatment with FMC in U-937 and HL-60 cells. To determine whether the chalcone induced cleavage of poly(ADP-ribose) polymerase (PARP), which is considered a hallmark of apoptosis and that indicates activation of caspase, nuclear fractions of treated cells were analyzed by immunoblotting. As shown, the 85 kDa fragment generated from the full-length PARP protein was detected in FMC-treated cells after 6 h exposure at a concentration as low as 1 μ M and increased in a concentration- and time-dependent manner (Figure 5b). Processing of caspases in cells treated with FMC were analyzed by immunoblotting to define the temporal relationship of caspase activation and PARP cleavage. Executioner caspases-3 and -7 were processed and detected by the generation of a fragment and a decrease of the proenzyme, respectively. The decrease of procaspase-7 was more evident in U-937 than in HL-60. Caspase-4 which is involved in inflammation was also examined and it was detected a decrease of the proenzyme after treatment with 3 μ M FMC in both cell lines. The initiator caspases were also processed and procaspase-9 processing was earlier than procaspase-8. The processing of caspase-9, detected as a decrease on the proenzyme, was observed at 6 h, whereas the decrease in the proenzymes procaspase-8 and -7 was detected after 12 h of treatment, at least in U-937 cells when PARP cleavage was more apparent. The levels of procaspase-9 processing peaked at 6 h, whereas the levels of cleaved caspase-3 peaked at 24 h. These cleavage patterns suggest that the initial PARP cleavage before caspase-3 cleavage might be attributable to caspase-9/caspase-7 cleavage, and then caspase-3 activation could amplify the hydrolysis of PARP.

To determine whether cell death triggered by FMC is blocked by a pan-caspase inhibitor, U-937 cells were pretreated with z-VAD-fmk (100 μ M) and then with the chalcone for 24 h and analyzed by flow cytometry after double staining with annexin V-FITC and propidium iodide. Results revealed that the general inhibitor decreased the percentage of annexin V-FITC positive cells as well as the percentage of propidium iodide positive cells (Figure 5c). As shown in Figure 5d, the percentage of annexin V-FITC plus propidium iodide positive cells was $4.3 \pm 0.3\%$ in control cells, which increased until $50.0 \pm 5.0\%$ after treatment with FMC or until $22.4 \pm 7.3\%$ in the combination group (z-VAD-fmk+FMC).

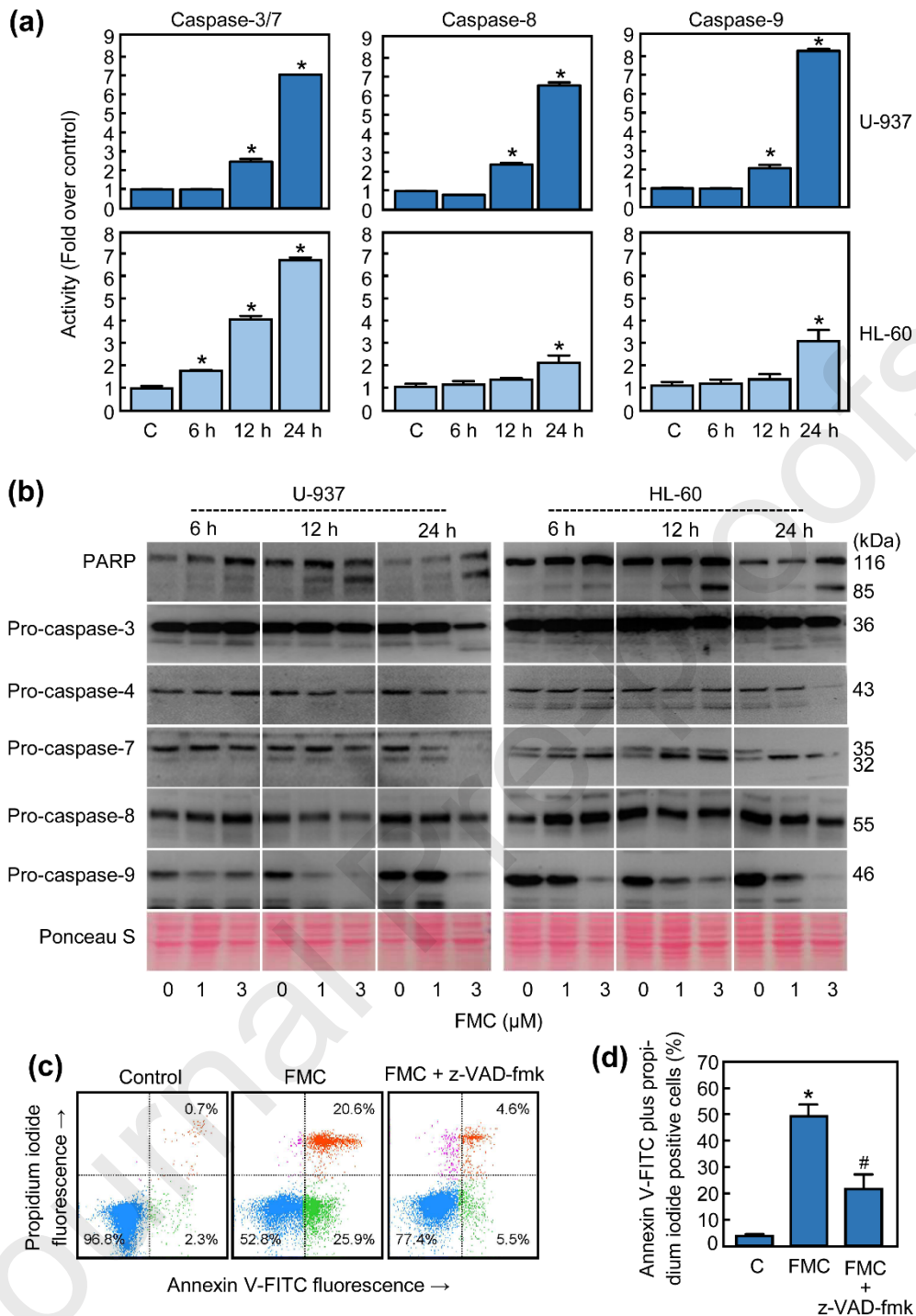


Figure 5. FMC induced caspase activation in human U-937 and HL-60 cells. (a) Time-course of caspase substrate hydrolysis activities. Cells were treated with 3 μ M FMC, harvested at indicated times and total cell lysates were assayed for caspase activity using the chromogenic substrates DEVD-*p*NA (for caspase-3/7), IETD-*p*NA (for caspase-8), and LEHD-*p*NA (for caspase-9). Results are expressed as fold increase in enzyme activity compared with control. Values represent means \pm SEs of two independent experiments performed in triplicate. (b) Time course of poly(ADP-ribose) polymerase (PARP) cleavage and procaspases processing. Cells were incubated with the indicated times and concentrations of FMC and proteins were detected by western blot. Ponceau S was used as a loading and transfer control. (c) U-937 cells were treated with FMC (3 μ M, 24 h) in the absence or the presence of z-VAD-fmk (100 μ M) and subjected to flow cytometry after double staining with annexin V-FITC and propidium iodide. (d) U-937 cells were treated as in (c) and quantified by flow cytometry. Bars represent means \pm SE of two independent experiments

performed in duplicate. * $P < 0.05$ from untreated control. # $P < 0.05$ significantly different from FMC treatment.

2.2.4. Furoxyloxychalcone induced cytochrome *c* release but did not decrease the mitochondrial membrane potential

Activation of caspase-9 is dependent on the release of cytochrome *c* from mitochondria to cytosol. To determine whether FMC-induced cell death involves cytochrome *c* release, dose-response and time-course experiments were performed and cytosolic fractions were analyzed by immunoblotting. As shown in Figure 6a, an increase in cytochrome *c* in the cytosol was detected starting at 6 h of treatment with a low concentration of FMC (1 μM) in both cell lines, U-937 and HL-60. To investigate whether a disruption of the mitochondrial membrane potential ($\Delta\Psi\text{m}$) is required for cytochrome *c* release, cells were treated with vehicle (DMSO) or increasing concentrations of FMC for 6 h, stained with the fluorochrome JC-1 and analyzed by flow cytometry. The results showed that $\Delta\Psi\text{m}$ remained intact for at least 6 h of treatment, suggesting that the dissipation of the mitochondrial membrane potential was not implicated in FMC-induced cell death (Figure 6b).

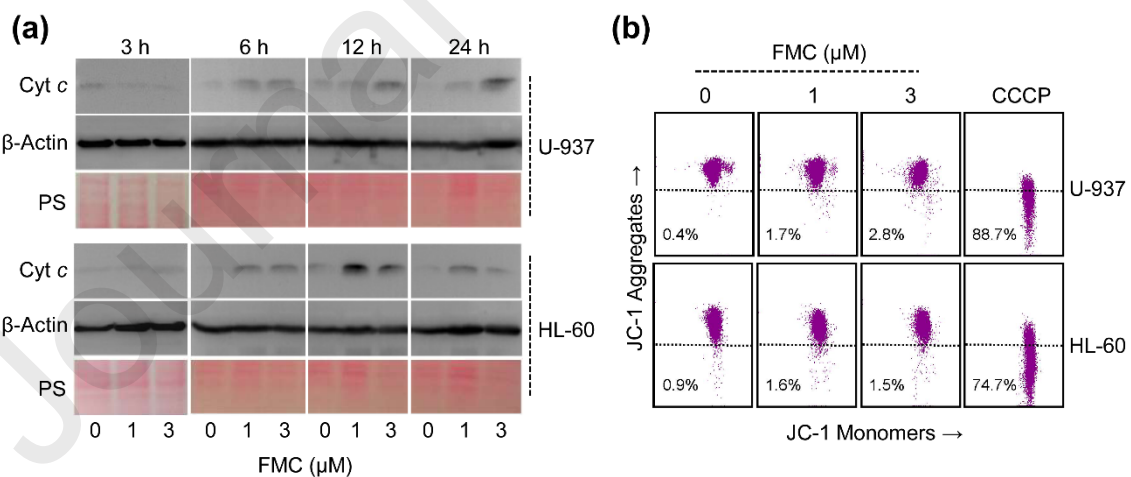


Figure 6. FMC induced cytochrome *c* release and did not reduce the mitochondrial membrane potential. (a) Representative immunoblots show the time- and concentration-dependent cytochrome *c* release by FMC. Cells were cultured with the specified concentrations of FMC for the indicated time points and cytosolic fractions were obtained and analyzed on Western blots with specific antibodies against cytochrome *c* and β -actin, which was used as a loading control. Equal protein loading was also controlled by staining the membrane with Ponceau S (PS) before the immunodetection. (b) Cells were incubated with the indicated concentrations of FMC for 6 h, stained with the JC-1 probe and $\Delta\Psi\text{m}$ was analyzed by flow cytometry. Similar results were obtained in two independent experiments each performed in triplicate. The protonophore CCCP (carbonyl cyanide *m*-chlorophenylhydrazone, 50 μM) was used as a positive control.

2.2.5. Overexpression of Bcl-2 confers protection against apoptosis induced by the *Furoyloxychalcone*

To confirm the key role of the intrinsic pathway in the mechanism of FMC-induced cell death, we compared the effect on apoptosis induction in U-937 cells over-expressing Bcl-2 (U-937/Bcl-2) and the parental U-937 cells. As shown in Figure 7a, dose-response experiments revealed that the over-expression of Bcl-2 almost completely suppressed the increase in the percentage of sub-G₁ cells after 24 h of treatment. U-937/Bcl-2 cells were, however, sensitive to cell cycle arrest at G₂-M phase induced by FMC (Figure 7b). The effect of FMC on cell viability was also evaluated in both cell lines and as expected, the reduction in the number of cells was higher in U-937 than in U-937/Bcl-2 (Figure 7c). The decrease in the number cells with respect to control in U-937/Bcl-2 may be a consequence of the G₂-M cell cycle arrest since in these conditions the percentage of viable cells was 96%. The cytotoxic agent ara-C (1-β-D-arabinofuranosylcytosine) which induces cell death through the mitochondrial pathway triggered a higher decrease in the number of cells in U-937 cells than in U-937/Bcl-2. The morphological changes and the decrease in the number of cells by FMC were clearly visualized by phase-contrast microscopy (Figure 7d).

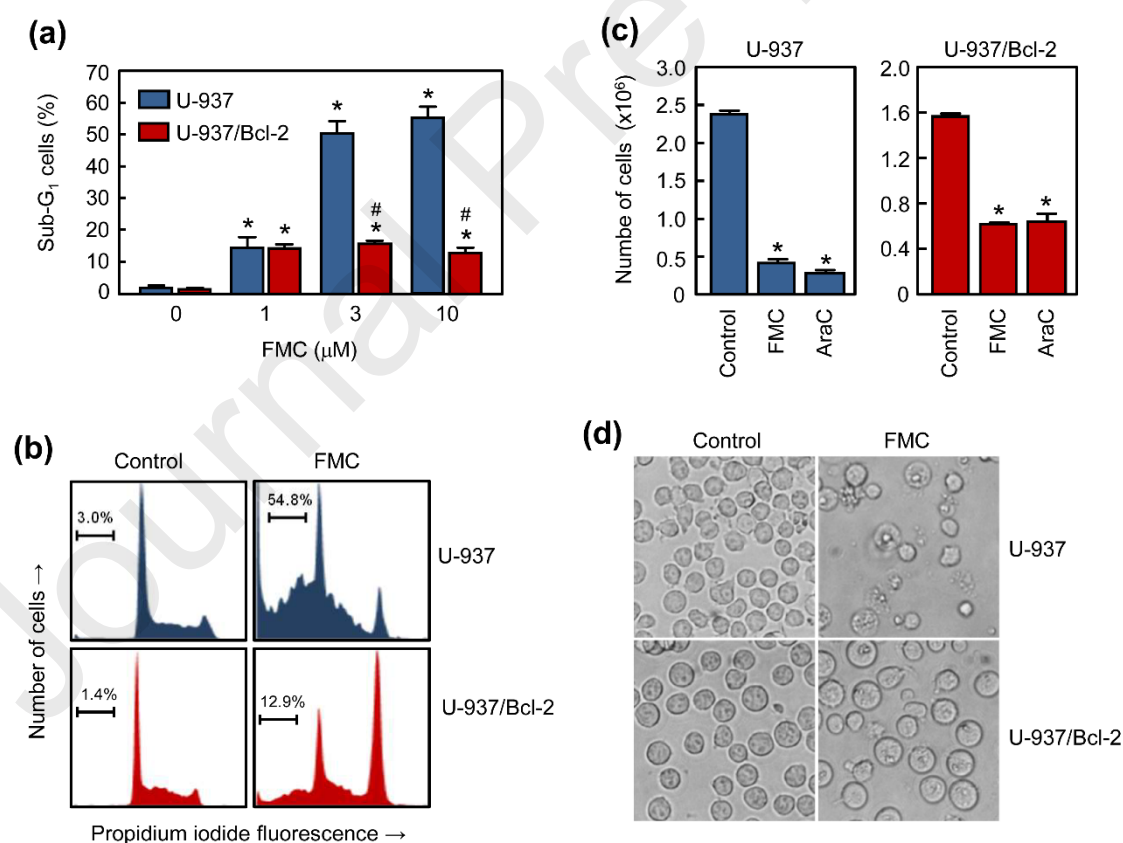


Figure 7. Over-expression of Bcl-2 blocked FMC-induced apoptosis. (a) Cells were cultured with the specified concentrations of FMC for 24 h and cell cycle analyzed by flow cytometry. (b) Representative histograms and the percentage of sub-G₁ cells (apoptotic cells) after treatment with 3 μM for 24 h are shown. (c) Differential effects on cell numbers after treatment with 3 μM FMC for 24 h. Ara-C (1-β-D-

arabinofuranosylcytosine, 1 μ M, 24 h) was included as a positive control. (d) Photomicrographs obtained with an inverted phase-contrast microscope after treatment with 3 μ M FMC for 24 h. * $P < 0.05$ from untreated control. # $P < 0.05$ significantly different from FMC treatment.

2.2.6. *Furoyloxychalcone induced downregulation of Bcl-xL and Mcl-1 and up-regulation of DR5*

To determine whether the inhibition of viability triggered by FMC was associated with changes in the expression of the Bcl-2 family proteins, cells were incubated with increasing concentrations of chalcone in time course experiments and whole cell lysates (or the cytosolic fraction in the case of Bax) were analyzed by immunoblotting. As shown in Figure 8, downregulation of Bcl-xL, Mcl-1 and cytosolic Bax was detected after 24 h of treatment with FMC. Although changes in the expression of the anti-apoptotic protein Bcl-2 were not observed, the levels of the pro-apoptotic Bak increased at 6 h of treatment at least in U-937 cells, while the pro-apoptotic members Bid and Bim decreased. In addition, the expression of TRAIL (Tumor Necrosis Factor-related apoptosis-inducing ligand) and death receptors which are involved in the extrinsic pathway of cell death were also explored. As shown in Figure 8, FMC failed to affect the expression levels of TRAIL, and appeared to decrease the levels of DR4 at least in U-937 cells. Interestingly, FMC increased the amounts of DR5 in both cell lines.

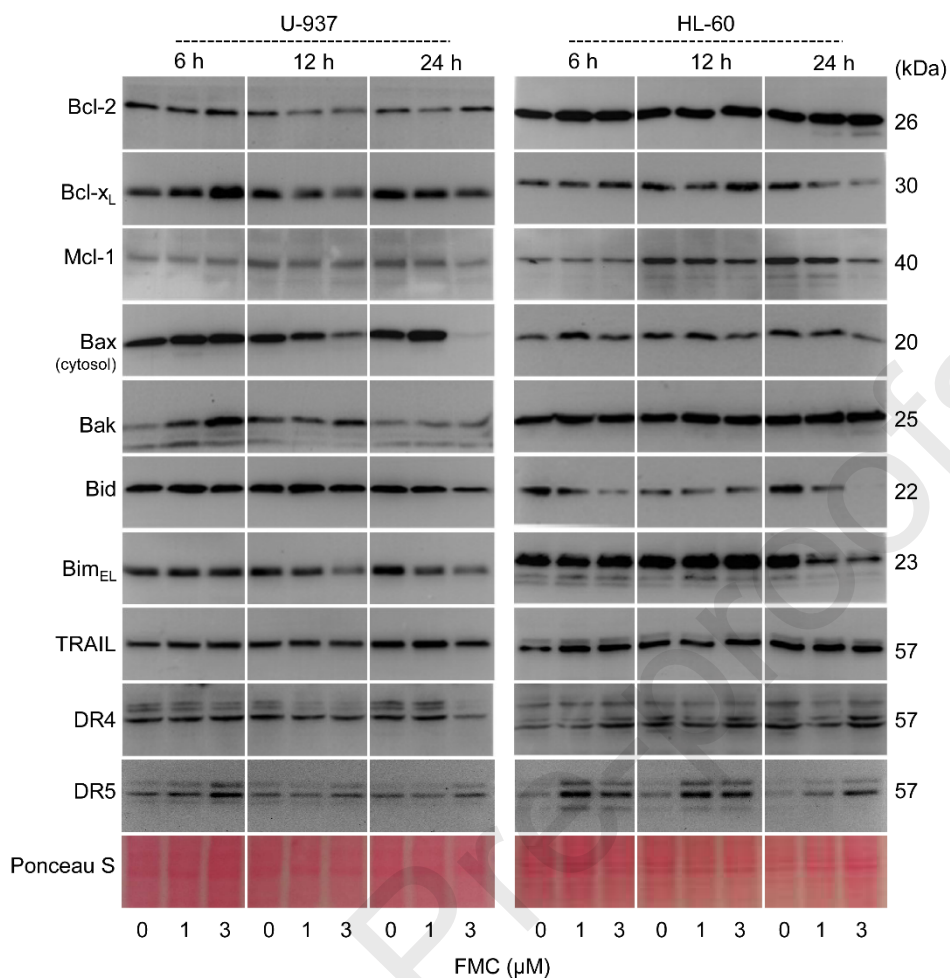


Figure 8. FMC induced changes in BCL-2 family proteins expression, TRAIL and Death Receptors. Cells were treated with the indicated concentrations of FMC for the specified times and whole cell lysates or cytosolic fractions (in the case of Bax) were subjected to immunoblotting. Ponceau S was used as a loading and transfer control. A representative section of the membrane is shown.

2.2.7. Furoxyloxychalcone increased reactive oxygen species generation and cell death was blocked by catalase and associated with MAPK pathway activation.

An increase in reactive oxygen species (ROS) may induce death in leukaemia cells [21]. To explore whether FMC induces ROS in U-937 and HL-60, cells were treated with the chalcone, stained with the fluorescent probe 2',7'-dichlorodihydrofluorescein diacetate (H₂DCF) and analyzed by flow cytometry. An increase in DCF fluorescence was detected in FMC-treated cells as detected by a rightward shift in fluorescence (Figure 9a). To investigate whether oxidative stress triggered by FMC is essential for FMC-mediated cell death, cells were pre-treated with catalase (500 units/mL), one of the most important antioxidants which has a crucial role in the degradation of H₂O₂. As shown, this enzyme was able to block in great part the increase in the percentage of sub-G₁ cells and the generation of ROS (Figures 9b and 9c). In addition, catalase

was found to at least partially block the reduction in the number of cells triggered by FMC (Figure 9d).

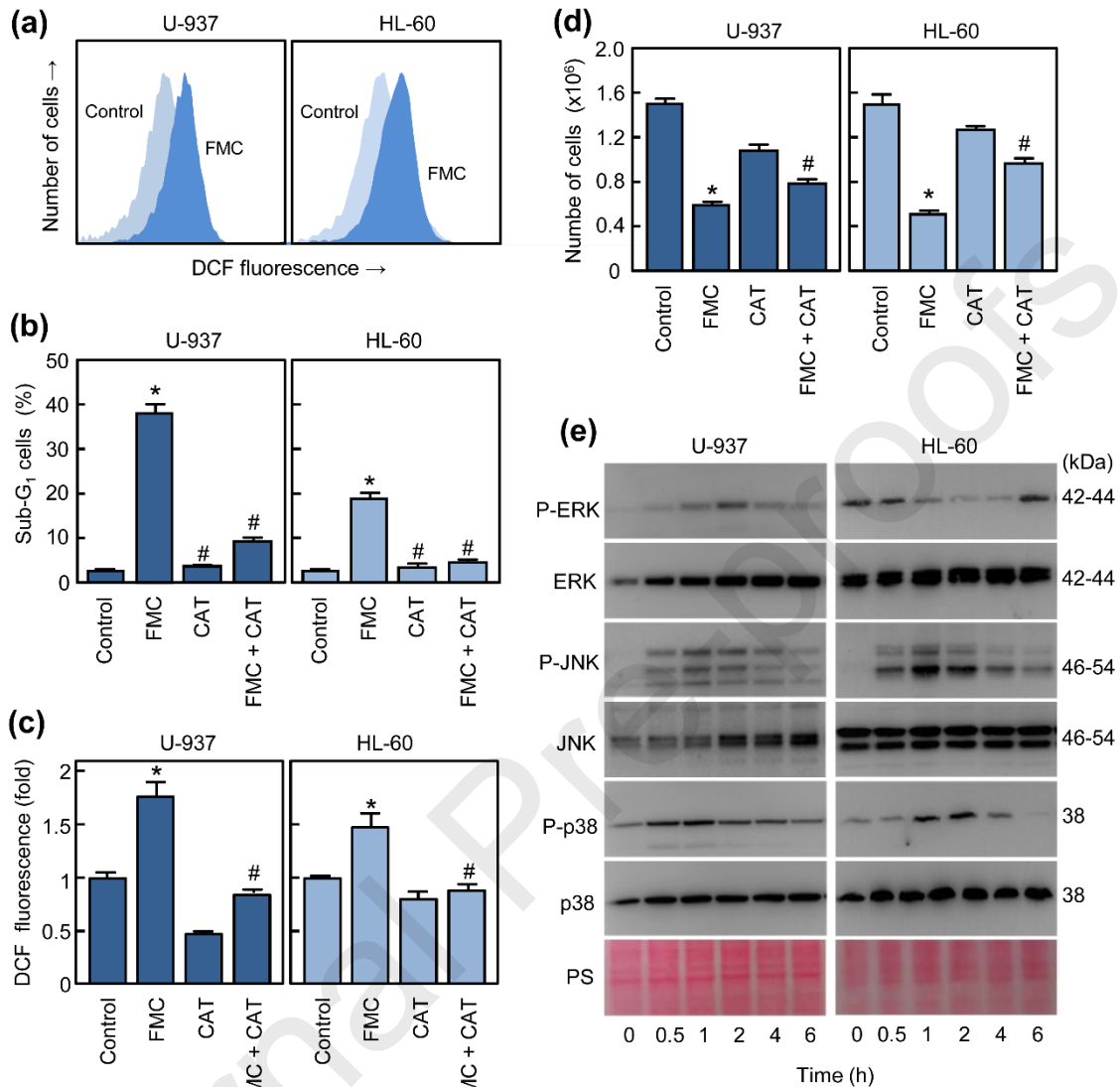


Figure 9. FMC induced ROS generation and MAPK activation. (a) Representative histograms of fluorescence obtained by flow cytometry after treatment with 3 μ M FMC for 3 h. (b) Cells were preincubated with catalase (CAT, 500 UI/mL) for 1 h and then treated for 24 h with 3 μ M FMC and the percentage of sub-G₁ cells was determined by flow cytometry. (c) Cells were preincubated with catalase for 1 h and then with 3 μ M FMC for 3 h and the fluorescence of oxidized H₂DCF was determined by flow cytometry. (d) Cells were treated as in (b) and the number of cells was determined by the trypan blue exclusion method. (e) Cells were treated with 3 μ M FMC for the specified times and MAPK phosphorylation was detected by immunoblotting. Membranes were stripped and reprobbed with total ERK, total JNK or total p38 antibodies as loading controls. Ponceau S (PS) staining was also used as alternative loading as well as transfer control. * $P < 0.05$ from untreated control. # $P < 0.05$ significantly different from FMC treatment.

Since the increase in ROS generation in leukemic cells lead to the activation of the mitogen-activated protein kinase (MAPK) cascade [21-24], the possibility that FMC was able to activate

this pathway was also investigated. As shown (Figure 9e), this chalcone lead to phosphorylation of *c-jun* *N*-terminal kinases/stress-activated protein kinases (JNK/SAPK) and p38^{MAPK} in U-937 and HL-60 cells, while phosphorylation of extracellular signal-regulated kinases 1/2 (ERK1/2) was only observed in U-937 cells.

3. Discussion

Few examples of chalcones containing the furoyloxy radical have been described to exhibit antiproliferative activity against cancer cell lines and display low cytotoxicity against normal cells [25]. In addition, chalcones containing specific aromatic rings have been tested as ABCG2 (ATP binding cassette G2) inhibitors [26]. In contrast, methoxyflavonoids have been described to be more potent inhibitors of cancer cell proliferation than their corresponding nonmethoxylated analogs [27]. The presence of methoxy groups or some lipophilic moieties in specific flavonoids confers hydrophobicity and significantly increases the potency and bioavailability and also enhances the stability and effectiveness by preventing chemical and metabolic hydrolysis [28-31].

In the present study, we attempted to find new potent antiproliferative molecules inspired by natural products. Specifically, we synthesized twelve chalcones and two cyclic compounds and evaluated the potential cytotoxicity against human tumour cells. The introduction of a furoyl heterocycle as an ester or an amide improved or maintained the cytotoxicity in most tumor cell lines and, in some cases, the observed increase in activity was highly significantly (compounds 2 and 4). Interestingly, the unavailability of intramolecular hydrogen bonding between the OH and the ketone group lead to an increase in cytotoxicity. This suggests that the ketone group would be free to interact with a specific binding site. This fact opens new avenues of research to unravel the mechanism of action.

The results revealed that a specific 4-methoxychalcone containing a furoyloxy radical at 2' position on the A ring (FMC) was the most cytotoxic compound, with IC₅₀ values of 0.2 ± 0.1 μM, 0.3 ± 0.1 μM and 0.6 ± 0.1 μM against U-937, HL-60 and MOLT-3 cells, respectively. Interestingly, the melanoma cell line MEL-HO was also sensitive to the antiproliferative effects

of this chalcone. To our knowledge this is the first time to date that the reduction of viability and the mechanism involved in cancer cells death of this specific chalcone has been described.

The human leukaemia U-937 and HL-60 cells were more sensitive to FMC than quiescent PBMC and the fibroblast-like Vero cells, as determined by the MTT assay. This chalcone was able to induce a fast G₂-M phase cell cycle arrest, starting at 6 h, and followed by an increase in the percentage of sub-G₁ cells. The G₂-M arrest triggered by FMC might be explained by an inhibition of tubulin polymerization or by changes in the expression and/or activity of G₂-M cell cycle regulators. Tubulin is widely recognized as an attractive molecular target for potential anticancer agents. Some flavonoids display their antiproliferative activity by targeting microtubules through tubulin binding [32] and we have previously reported that some naturally occurring and synthetic flavonoids block tubulin polymerization [33-35]. Here we found that FMC inhibited tubulin polymerization in a concentration-dependent manner. This result revealed that FMC may target tubulin to exhibit cytotoxicity. Interestingly, this chalcone was able to induce the cyclin-dependent kinases (Cdk) inhibitor p21^{Cip1/WAF1}, suggesting a relationship between the G₂-M arrest and cell death induction. Future studies will be needed to determine the effect of FMC on additional G₂-M cell cycle regulators such as Cdk1, B-type cyclin isoforms and Cdc25C phosphatase.

The synthetic chalcone induced the activation and processing of initiator and executioner caspases in U-937 and HL-60 cells. The temporal relationship between caspase activation and PARP cleavage suggests that the initial PARP hydrolysis might be due to caspase-9/caspase-7 cleavage, followed by caspase-3 activation which could amplify the processing of PARP. Cell death induced by FMC was dependent on caspases since the general inhibitor of caspases, z-VAD-fmk, was able to significantly decrease the percentage of annexin V-FITC positive cells at least in U-937 cells. The furoxyloxychalcone FMC induced an early release of cytochrome *c* (6 h) and this was not accompanied by dissipation of the mitochondrial transmembrane potential. Our results are in accordance with previous studies on cell lines indicating that mitochondrial events associated with changes in $\Delta\Psi_m$ are not required for the complete release of cytochrome *c* upon mitochondrial outer membrane permeabilization [36]. Apoptosis without complete mitochondrial

potential dissipation has also been reported to occur in CEM cells [37]. The absence of a parallel decrease in $\Delta\Psi_m$ and the cytochrome *c* release observed in HL-60 and U-937 cells might be explained by the possibility that not all mitochondrial cytochrome *c* actively participates in the electron transport chain, as previously suggested by Bossy-Wetzel et al. [37]. Whether FMC promotes mitochondrial $\Delta\Psi_m$ dissipation, particularly at longer times of treatment, cannot be ruled out.

Overexpression of the anti-apoptotic protein Bcl-2 blocked the cell death triggered by FMC which suggests that Bcl-2 itself might be a potential target in the mechanism of cell death. Although FMC failed to down-regulate the Bcl-2 protein, the furoxyloxychalcone downregulated the levels of the anti-apoptotic proteins Bcl-xL and Mcl-1 after 24 h of treatment. Furthermore, cytosolic levels of Bax were decreased suggesting a translocation of Bax to mitochondrial outer membrane in accordance upon apoptosis induction. The immunoblot experiments revealed a downregulation of Bid which might be caused by truncation of the full-length Bid by caspase-8 activation and processing. The activation of this initiator caspase is mediated by ligand-binding to death receptors and activation of the death-domain-containing tumor necrosis factor receptor superfamily. The results revealed that FMC is a DR5 inducer and may have potential clinical importance, however further research is needed to determine whether this chalcone is able to amplify the sensitivity to TRAIL.

The generation of ROS causes oxidative stress and cell death [38]. In this paper, we demonstrated that FMC increased the levels of ROS in U-937 and HL-60 cells. Although we have not identified the primary source of ROS, we demonstrated that ROS generation was an early event since it was detected after 3 h of treatment with FMC. In contrast, the release of cytochrome *c* was not detected until 6 h of treatment. Time course experiments of cytochrome *c* release in both cell lines revealed the absence of cytochrome *c* in the cytosol of U-937 and HL-60 cells at 3 h of treatment. Thus, ROS generation appears not to be a consequence of cytochrome *c* release. Interestingly, the generation of ROS as well as the increase in the percentage of sub-G₁ cells was reversed by the antioxidant enzyme catalase suggesting that the oxidative stress triggered by FMC is involved in the mechanism of cell death. Furthermore, FMC was able to activate the mitogen-activated protein

kinase (MAPK) signaling pathway which is involved in cell proliferation, survival and death [39]. Specifically, FMC induced the phosphorylation and activation of the JNK/SAPK and p38^{MAPK} in both cell lines. Future experiments will be necessary to determine the role of these protein kinases in the mechanism of cell death.

4. Conclusions

In summary, we designed and synthesized a series of chalcones including two cyclic compounds either with or without a furoyl radical and evaluated their cytotoxicity against five human tumor cell lines. The SARs revealed that (i) the presence of a 2' amino group in 4-methoxychalcone generated a more cytotoxic compound than the corresponding 2'-hydroxy against leukemic cells, and the introduction of a furoyl radical in position 2' as an ester or an amide group enhanced the cytotoxicity against leukaemia and melanoma cells; and (ii) the substitution of 2'-hydroxy for a 2'-amino group in 3,4,5-trimethoxychalcones enhanced the cytotoxicity against leukaemia and melanoma cells but the corresponding furoyl derivatives did not enhance the cytotoxicity as in the case of 4-methoxychalcones. The 4-methoxychalcone containing a furoyloxy radical at 2' on the A ring (FMC) was one of the most potent cytotoxic compound of this series against the human leukaemia U-937, HL-60, MOLT-3 cells and the human melanoma cell line MEL-HO. Interestingly, FMC showed less cytotoxic potential against normal cells, as the human peripheral blood mononuclear cells and the fibroblast-like Vero cells, suggesting that this compound may have therapeutic potential. FMC arrested the cells in the G₂-M phase, induced the cell cycle inhibitor p21^{Cip1/WAF1} and inhibited the polymerization of tubulin. Cell death induced by FMC was associated with caspase activation, PARP cleavage, cytochrome *c* release from mitochondria, induction of the Death Receptor 5, changes in Bcl-2 family proteins expression and the over-expression of the anti-apoptotic protein Bcl-2 blocked the increase in the percentage of sub-G₁ cells. The mechanism of cell death appeared to be related to the generation of reactive oxygen species (ROS) since FMC induced ROS and the antioxidant enzyme catalase was able to block ROS and cell death.

5. Material and methods

5.1. General Method and Reagents

^1H and ^{13}C NMR spectra were obtained on a Bruker Ascen 400 spectrometer model with standard pulse sequences operating at 400 MHz in ^1H and 101 MHz in ^{13}C NMR. Chemical shifts (δ) are given in ppm upfield from tetramethylsilane as internal standard. Coupling constants (J) are reported in hertz. EIMS and HREIMS were recorded on a Micromass model Autospec (70 eV) spectrometer. Column chromatography was carried out on silica gel 60 (Merck 230–400 mesh) and analytical thin layer chromatography (TLC) was performed using silica gel aluminum sheets. The general inhibitor of caspases z-VAD-fmk [benzyloxycarbonyl-Val-Ala-Asp(OMe) fluoromethyl ketone] was from Calbiochem (Darmstadt, Germany). Ammonium persulfate, acrylamide, bisacrylamide and N,N,N',N' -tetramethylethylenediamine were from Bio-Rad (Hercules, CA, USA). Poly(vinylidene difluoride) membranes and Immobilon Western Chemiluminiscent HRP Substrate were from Millipore (Billerica, MA, USA). All other chemicals were obtained from Sigma (Saint Louis, MO, USA). The primary antibodies used for immunoblots were obtained from the following companies (all at 1:1,000 dilution): anti-Bak (#12105), anti-Bax (#2772), anti-Bcl-2 (#4223), anti-Bcl-xL (#2764), anti-Bid (#2002), anti-Bim (#2933), anti-caspase-7 (#9494), anti-caspase-8 (#9746), anti-caspase-9 (#9502), anti-Mcl-1 (#4572), anti-JNK/SAPK (#9252), anti-phospho-JNK/SAPK (phosphor T183 + Y185) (#9251), anti-p44/42 MAP Kinase (ERK1/2) (#9102), anti-phospho-p44/42 MAPK (Erk1/2) (Thr202/Tyr204) (#9101), anti-p38^{MAPK} (#9212), anti-phospho-p38^{MAPK} (T180/Y182) (#9211), anti-p21 (#2947) and anti- α -tubulin (#2125) antibodies from Cell Signaling Technology (Beverly, MA, USA). Anti-caspase-3 (#ADI-AAP-113) was from Enzo (Ann Arbor, MI, USA); anti-cytochrome *c* (556433) and anti-PARP [poly(ADP-ribose) polymerase] (#551024) were from BD Pharmingen (San Diego, CA, USA); anti-DR4 (ab8414), anti-DR5 (ab47179) and anti-TRAIL (ab9959) were from Abcam (Cambridge, UK). Alexa Fluor 594-conjugated goat anti-rabbit antibody (#A-11012) was from Invitrogen (Eugene, OR, USA). Anti- β -actin (clone AC-74, A2228) was from Sigma-Aldrich (Saint Louis, MO, USA); Horseradish peroxidase-conjugated

secondary antibodies (NA9310 and NA9340) from GE Healthcare (Little Chalfont, UK) were used at 1:10,000 dilution.

5.2. General procedure for the synthesis of chalcones (1, 3, 5, 7, 9, 11)

A mixture of the acetophenone (5-10 mmol, 1 equiv) and the corresponding benzaldehyde (1 equiv) in EtOH (20-40 mL) was stirred at room temperature and a 50% aqueous solution of NaOH (5-8 mL) was added. The reaction mixture was stirred at room temperature until the starting materials had been consumed. HCl (10%) was then added until neutrality. Precipitated chalcones were generally filtered and crystallized from MeOH, although in some cases the product was purified using column chromatography.

5.3. General procedure for the synthesis of furoyl derivatives (2, 4, 6, 8, 10, 12, 14)

Furoyl chloride (1.1 equiv) was added, at room temperature under argon, to a solution of 2'-hydroxychalcone (approx. 0.05 mmol, 1.0 equiv) and triethylamine (1.5 equiv) in dry CH₂Cl₂ (0.1 M). After being stirred for 6 h, the reaction mixture was quenched with saturated aqueous NH₄Cl. The organic layer was separated and the aqueous layer was extracted twice with CH₂Cl₂. The combined organic layers were washed twice with saturated aqueous NaHCO₃, dried over MgSO₄ and filtered. The filtrate was concentrated in vacuum, and then the resulting residue was purified by column chromatography (eluted with Hex:Ethyl Acetate = 3:1) on silica gel to afford the furoyl derivatives (2, 4, 6, 8, 10, 12 and 14).

5.4. Procedure for the synthesis of flavonol (13)

A solution of the 2-hydroxychalcone **1** (0.1-0.2 mmol) in 3.0 M KOH in MeOH (2-3 mL) was cooled at 0 °C. An aqueous solution of H₂O₂ (30%) (0.5 mL) was added to the chalcone solution. The resulting mixture was stirred at room temperature, until the starting material was totally consumed (as evidenced by TLC). The reaction mixture was cooled in an ice bath and distilled water (2-4 mL) was added together with HCl (2 M) until pH 2. The precipitate was filtered and washed with distilled water and recrystallized from MeOH.

5.5. Spectroscopic data of compounds 1-14

5.5.1. (*E*)-1-(2-hydroxyphenyl)-3-(4-methoxyphenyl)prop-2-en-1-one (**1**): Orange amorphous solid (82%). ^1H NMR (500 MHz, CDCl_3) δ 7.67 (d, $J = 16.2$ Hz, 1H),

7.62 (dd, $J = 1.8, 0.9$ Hz, 1H), 7.51 (dd, $J = 7.9, 1.5$ Hz, 1H), 7.48-7.38

(m, 2H), 7.38-7.32 (m, 2H), 7.30 (dd, $J = 3.5, 0.9$ Hz, 1H), 7.29-7.22

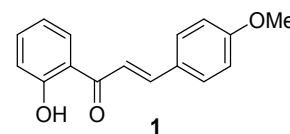
(m, 3H), 7.17 (dd, $J = 8.1, 1.1$ Hz, 1H), 7.15-7.09 (m, 1H), 7.06 (d, $J = 16.2$ Hz, 1H), 6.99 (dd, J

$= 8.2, 0.8$ Hz, 1H), 6.97 (dd, $J = 8.4, 0.8$ Hz, 1H), 6.54 (dd, $J = 3.6, 1.7$ Hz, 1H), 5.17 (s, 2H). ^{13}C

NMR (126 MHz, CDCl_3) δ 192.2, 156.9, 156.3, 148.1, 147.3, 143.5, 139.5, 139.4, 136.2, 131.4,

131.0, 129.2, 128.5, 128.4, 127.9, 127.0, 126.2, 124.8, 123.3, 119.8, 118.7, 115.6, 112.1, 110.5,

70.7. HRMS (ESI-FT-ICR) m/z : 277.0846 [$\text{M}+\text{Na}$]; calcd. for $\text{C}_{16}\text{H}_{14}\text{NaO}_3$: 277.0837.



5.5.2. (*E*)-2-[3-(4-methoxyphenyl)acryloyl]phenyl furan-2-carboxylate (**2**): Yellow oil (60%). ^1H

NMR (500 MHz, CDCl_3) δ 7.73 (dd, $J = 7.7, 1.7$ Hz, 1H), 7.62-

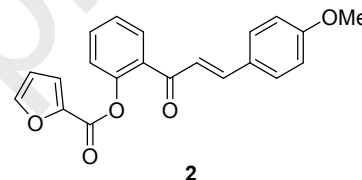
7.51 (m, 3H), 7.48-7.41 (m, 2H), 7.39 (td, $J = 7.5, 1.1$ Hz, 1H),

7.34-7.28 (m, 2H), 7.07 (d, $J = 15.9$ Hz, 1H), 6.90-6.81 (m, 2H),

6.49 (dd, $J = 3.5, 1.7$ Hz, 1H), 3.83 (s, 3H). ^{13}C NMR (126 MHz, CDCl_3) δ 191.4, 161.7, 156.5,

148.0, 147.2, 145.4, 143.6, 132.8, 132.2, 130.2, 129.9, 127.2, 126.2, 123.3, 123.3, 119.9, 114.3,

112.2, 55.4. HRMS (ESI-FT-ICR) m/z : 371.0897 [$\text{M}+\text{Na}$]; calcd. for $\text{C}_{21}\text{H}_{16}\text{NaO}_5$: 371.0895.



5.5.3. (*E*)-1-(2-aminophenyl)-3-(4-methoxyphenyl)prop-2-en-1-one (**3**): Orange amorphous solid (75%). ^1H NMR (400 MHz, CDCl_3) δ 7.86 (dd, $J = 8.3, 1.6$ Hz, 1H),

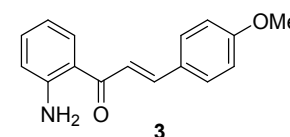
7.72 (d, $J = 15.5$ Hz, 1H), 7.59 (d, $J = 8.7$ Hz, 2H), 7.50 (d, $J = 15.5$

Hz, 1H), 7.33-7.23 (m, 1H), 6.93 (d, $J = 8.8$ Hz, 2H), 6.74-6.65 (m, 2H), 6.30 (s, 2H), 3.85 (s,

3H). ^{13}C NMR (101 MHz, CDCl_3) δ 191.8, 161.3, 150.8, 142.8, 134.1, 130.9, 129.9, 128.0, 120.8,

119.3, 117.2, 115.8, 114.3, 55.4. HRMS (ESI-FT-ICR) m/z : 276.0998 [$\text{M}+\text{Na}$]; calcd. for

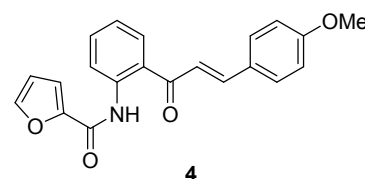
$\text{C}_{16}\text{H}_{15}\text{NNaO}_2$: 276.1000.



5.5.4. (*E*)-*N*-{2-[3-(4-methoxyphenyl)acryloyl]phenyl}furan-2-carboxamide (**4**): Yellow amorphous solid (68%). ^1H NMR (400 MHz, CDCl_3) δ 12.57 (s,

1H), 8.87 (dd, $J = 8.5, 1.2$ Hz, 1H), 8.03 (dd, $J = 8.0, 1.6$ Hz, 1H),

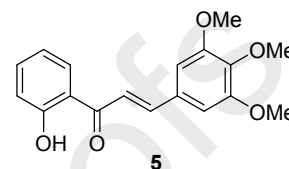
7.87 (d, $J = 15.5$ Hz, 1H), 7.69-7.55 (m, 4H), 7.49 (d, $J = 15.5$ Hz,



1H), 7.28 (dd, $J = 3.5, 0.9$ Hz, 1H), 7.20 (ddd, $J = 8.2, 7.3, 1.2$ Hz, 1H), 6.95 (d, $J = 8.8$ Hz, 2H), 6.56 (dd, $J = 3.5, 1.7$ Hz, 1H), 3.87 (s, 3H). ^{13}C NMR (101 MHz, CDCl_3) δ 193.3, 162.0, 156.9, 148.3, 145.6, 144.9, 140.7, 134.5, 130.5, 130.4, 127.4, 123.9, 122.6, 121.2, 120.3, 115.3, 114.5, 112.2, 55.4. HRMS (ESI-FT-ICR) m/z : 385.0681 [M+Na]; calcd. for $\text{C}_{21}\text{H}_{14}\text{NaO}_6$: 385.0688

5.5.5. (*E*)-1-(2-hydroxyphenyl)-3-(3,4,5-trimethoxyphenyl)prop-2-en-1-one (5): Orange amorphous solid (77%). ^1H NMR (500 MHz, CDCl_3) δ 12.84 (s, 1H),

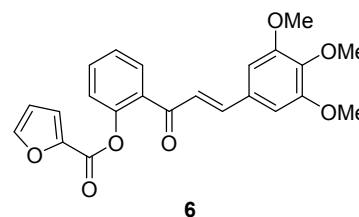
7.94 (dd, $J = 8.0, 1.6$ Hz, 1H), 7.85 (d, $J = 15.4$ Hz, 1H), 7.57-7.48 (m, 2H), 7.04 (dd, $J = 8.4, 1.2$ Hz, 1H), 6.96 (ddd, $J = 8.2, 7.1, 1.2$ Hz, 1H),



6.89 (s, 2H), 3.94 (s, 6H), 3.92 (s, 3H). ^{13}C NMR (101 MHz, CDCl_3) δ 193.5, 163.6, 153.5, 145.6, 140.8, 136.3, 130.0, 129.6, 120.0, 119.3, 118.8, 118.6, 105.9, 61.0, 56.3. HRMS (ESI-FT-ICR) m/z : 337.1046 [M+Na]; calcd. for $\text{C}_{18}\text{H}_{18}\text{NaO}_5$: 337.1052.

5.5.6. (*E*)-2-[3-(3,4,5-trimethoxyphenyl)acryloyl]phenyl furan-2-carboxylate (6): Yellow oil (55%). ^1H NMR (500 MHz, CDCl_3) δ 7.66 (dd, $J = 7.6, 1.7$ Hz,

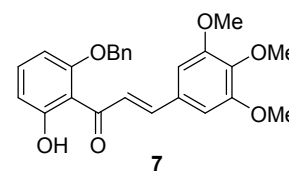
1H), 7.55-7.49 (m, 2H), 7.41 (d, $J = 15.9$ Hz, 1H), 7.34 (td, $J = 7.6, 1.1$ Hz, 1H), 7.29-7.22 (m, 2H), 6.99 (d, $J = 15.9$ Hz, 1H), 6.65 (s, 2H), 6.43 (dd, $J = 3.5, 1.7$ Hz, 1H), 3.81 (s, 3H), 3.78 (s,



6H). ^{13}C NMR (126 MHz, CDCl_3) δ 191.5, 161.8, 156.5, 153.4, 148.0, 147.3, 145.6, 143.6, 140.4, 132.6, 132.4, 129.9, 126.3, 125.0, 123.4, 120.0, 112.2, 105.6, 61.0, 56.1. HRMS (ESI-FT-ICR) m/z : 431.1093 [M+Na]; calcd. for $\text{C}_{23}\text{H}_{20}\text{NaO}_7$: 431.1107.

5.5.7. (*E*)-1-[2-(benzyloxy)-6-hydroxyphenyl]-3-(3,4,5-trimethoxyphenyl)prop-2-en-1-one (7): Yellow amorphous solid (75%). ^1H NMR (400 MHz, CDCl_3) δ 13.09

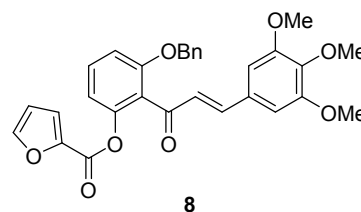
(s, 1H), 7.79 (d, $J = 15.5$ Hz, 1H), 7.72 (d, $J = 15.5$ Hz, 1H), 7.47-7.32 (m, 3H), 7.32-7.17 (m, 4H), 6.66 (dd, $J = 8.4, 1.0$ Hz, 1H), 6.62



(s, 2H), 6.54 (dd, $J = 8.3, 1.0$ Hz, 1H), 5.17 (s, 2H), 3.88 (s, 3H), 3.67 (s, 6H). ^{13}C NMR (101 MHz, CDCl_3) δ 194.3, 164.8, 160.0, 153.2, 143.1, 140.2, 135.9, 135.8, 130.5, 128.7, 128.2, 127.2, 127.0, 112.4, 111.3, 105.8, 102.7, 71.1, 60.9, 56.0. HRMS (ESI-FT-ICR) m/z : 443.1479 [M+Na]; calcd. for $\text{C}_{25}\text{H}_{24}\text{NaO}_6$: 443.1471.

5.5.8. (*E*)-3-(benzyloxy)-2-[3-(3,4,5-trimethoxyphenyl)acryloyl]phenyl furan-2-carboxylate (**8**):

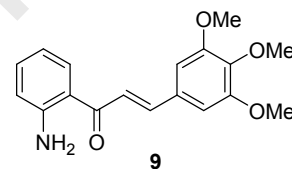
Pale yellow oil (48%). ¹H NMR (400 MHz, CDCl₃) δ 7.60 (dd, *J* = 1.8, 0.8 Hz, 1H), 7.42 (t, *J* = 8.3 Hz, 1H), 7.32 (dt, *J* = 6.0, 2.1 Hz, 3H), 7.29-7.27 (m, 2H), 7.25 (d, *J* = 7.2 Hz, 6H), 6.95 (dd, *J* = 8.4, 1.4 Hz, 2H), 6.89 (d, *J* = 16.1 Hz, 1H), 6.70 (s, 2H), 6.52



(dd, *J* = 3.5, 1.7 Hz, 1H), 5.14 (s, 2H), 3.87 (s, 3H), 3.83 (s, 6H). ¹³C NMR (101 MHz, CDCl₃) δ 192.3, 156.8, 156.4, 153.3, 147.9, 147.4, 146.2, 143.4, 140.3, 136.2, 130.8, 130.0, 128.5, 127.9, 127.3, 127.0, 123.4, 119.9, 115.5, 112.1, 110.5, 105.6, 70.6, 60.9, 56.1. HRMS (ESI-FT-ICR) *m/z*: 537.1528 [M+Na]; calcd. for C₃₀H₂₆NaO₈: 537.1525.

5.5.9. (*E*)-1-(2-aminophenyl)-3-(3,4,5-trimethoxyphenyl)prop-2-en-1-one (**9**): Orange

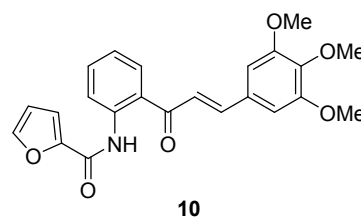
amorphous solid (78%). ¹H NMR (500 MHz, CDCl₃) δ 7.86 (dd, *J* = 8.4, 1.5 Hz, 1H), 7.65 (d, *J* = 15.4 Hz, 1H), 7.49 (d, *J* = 15.5 Hz, 1H), 7.30 (ddd, *J* = 8.4, 7.0, 1.5 Hz, 1H), 6.85 (s, 2H), 6.77-6.66 (m, 2H),



6.32 (s, 2H), 3.92 (s, 6H), 3.90 (s, 3H). ¹³C NMR (126 MHz, CDCl₃) δ 191.5, 153.4, 150.9, 143.1, 140.1, 134.2, 130.9, 130.8, 122.4, 119.1, 117.3, 115.8, 105.5, 61.0, 56.2. HRMS (ESI-FT-ICR) *m/z*: 314.1394 [M+H]; calcd. for C₁₈H₂₀NO₄: 314.1392.

5.5.10. (*E*)-*N*-{2-[3-(3,4,5-trimethoxyphenyl)acryloyl]phenyl}furan-2-carboxamide (**10**): Pale yellow oil (57%). ¹H NMR (500 MHz, CDCl₃) δ 12.51 (s, 1H),

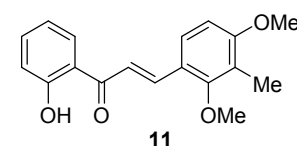
8.88 (dd, *J* = 8.4, 1.6 Hz, 1H), 8.03 (dd, *J* = 7.9, 1.6 Hz, 1H), 7.86-7.74 (m, 1H), 7.69-7.57 (m, 2H), 7.48 (dt, *J* = 15.4, 1.4 Hz, 1H), 7.28 (d, *J* = 3.5 Hz, 1H), 7.25-7.19 (m, 1H), 6.88 (t, *J* = 1.4



Hz, 2H), 6.57 (dd, *J* = 3.4, 1.7 Hz, 1H), 3.93 (s, 7H), 3.92 (s, 3H). ¹³C NMR (126 MHz, CDCl₃) δ 193.3, 156.9, 153.5, 148.3, 145.9, 145.0, 140.8, 140.7, 134.7, 130.6, 130.1, 123.7, 122.6, 122.0, 121.3, 115.4, 112.3, 105.8, 61.0, 56.2. HRMS (ESI-FT-ICR) *m/z*: 430.1362 [M+Na]; calcd. for C₂₃H₂₁NNaO₆: 430.1267.

5.5.11. (*E*)-3-(2,4-dimethoxy-3-methylphenyl)-1-(2-hydroxyphenyl)prop-2-en-1-one (**11**):

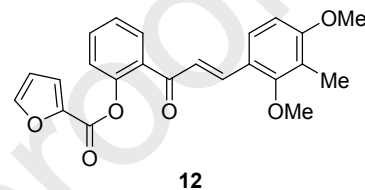
Yellow amorphous solid (84%). ¹H NMR (400 MHz, CDCl₃) δ 13.01



(s, 1H), 8.13 (d, $J = 15.5$ Hz, 1H), 7.93 (dd, $J = 8.1, 1.6$ Hz, 1H), 7.71 (d, $J = 15.5$ Hz, 1H), 7.55 (d, $J = 8.7$ Hz, 1H), 7.48 (ddd, $J = 8.6, 7.2, 1.6$ Hz, 1H), 7.02 (dd, $J = 8.4, 1.2$ Hz, 1H), 6.93 (ddd, $J = 8.2, 7.2, 1.2$ Hz, 1H), 6.72 (d, $J = 8.6$ Hz, 1H), 3.89 (s, 3H), 3.79 (s, 3H), 2.19 (s, 3H). ^{13}C NMR (101 MHz, CDCl_3) δ 194.1, 163.5, 161.3, 159.6, 141.4, 136.0, 129.5, 127.4, 120.8, 120.6, 120.2, 118.7 (x2), 118.5, 106.6, 61.5, 55.8, 8.94. HRMS (ESI-FT-ICR) m/z : 430.1362 [M+Na]; calcd. for $\text{C}_{23}\text{H}_{21}\text{NNaO}_6$: 430.1267.

5.5.12. (*E*)-2-[3-(2,4-dimethoxy-3-methylphenyl) acryloyl]phenyl furan-2-carboxylate (**12**): Pale yellow oil (42%). ^1H NMR (400 MHz, CDCl_3) δ 7.80 (d, $J = 16.0$

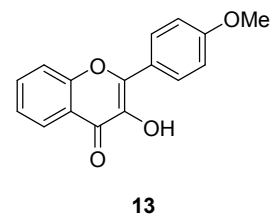
Hz, 1H), 7.73 (dd, $J = 7.7, 1.7$ Hz, 1H), 7.61-7.53 (m, 2H), 7.42-7.35 (m, 2H), 7.35-7.29 (m, 2H), 7.16 (d, $J = 16.0$ Hz, 1H), 6.63



(d, $J = 8.7$ Hz, 1H), 6.50 (dd, $J = 3.6, 1.7$ Hz, 1H), 3.86 (s, 3H), 3.66 (s, 3H), 2.13 (s, 3H). ^{13}C NMR (101 MHz, CDCl_3) δ 191.8, 161.0, 159.3, 156.5, 148.0, 147.2, 143.7, 141.4, 132.9, 132.1, 129.9, 126.5, 126.1, 124.2, 123.3, 120.7, 120.3, 119.8, 112.1, 106.5, 61.5, 55.7, 8.8. HRMS (ESI-FT-ICR) m/z : 415.1154 [M+Na]; calcd. for $\text{C}_{23}\text{H}_{20}\text{NaO}_6$: 415.1158.

5.5.13. 3-hydroxy-2-(4-methoxyphenyl)-4H-chromen-4-one (**13**): Pale yellow amorphous solid (79%). ^1H NMR (400 MHz, CDCl_3) δ 8.25 (d, $J = 9.0$ Hz, 3H), 7.70 (ddd,

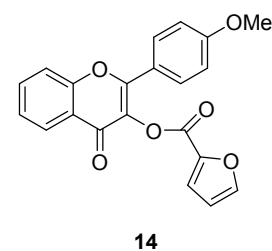
$J = 8.6, 7.0, 1.7$ Hz, 1H), 7.58 (dd, $J = 8.5, 1.1$ Hz, 1H), 7.41 (ddd, $J = 8.1, 7.0, 1.1$ Hz, 1H), 7.06 (d, $J = 9.1$ Hz, 2H), 6.96 (s, 1H), 3.90 (s, 3H).



^{13}C NMR (101 MHz, CDCl_3) δ 173.16, 161.12, 155.31, 145.34, 137.65, 133.38, 129.55, 125.42, 124.45, 123.56, 120.74, 118.20, 114.12, 55.44. HRMS (ESI-FT-ICR) m/z : 291.0633 [M+Na]; calcd. for $\text{C}_{16}\text{H}_{12}\text{NaO}_4$: 291.0633.

5.5.14. 2-(4-methoxyphenyl)-4-oxo-4H-chromen-3-yl furan-2-carboxylate (**14**): White amorphous solid (60%). ^1H NMR (400 MHz, CDCl_3) δ 8.27 (dd, $J = 8.0,$

1.7 Hz, 1H), 7.93 (d, $J = 9.0$ Hz, 2H), 7.76-7.65 (m, 2H), 7.57 (dd, $J = 8.5, 1.1$ Hz, 1H), 7.47-7.40 (m, 2H), 6.99 (d, $J = 9.0$ Hz, 2H), 6.60 (dd, $J = 3.6, 1.7$ Hz, 1H), 3.86 (s, 3H). ^{13}C NMR (101 MHz, CDCl_3) δ 171.8,



162.0, 156.4, 155.5, 155.4, 147.4, 143.4, 133.8, 132.5, 130.1, 126.2, 125.1, 123.6, 122.1, 120.3,

118.0, 114.2, 112.3, 55.4. HRMS (ESI-FT-ICR) m/z : 385.0681 [M+Na]; calcd. for $C_{21}H_{14}NaO_6$: 385.0688.

5.6. Cell culture

The human leukaemia U-937 (pro-monocytic, human myeloid leukaemia), HL-60 (acute myeloid leukaemia) and MOLT-3 (an acute lymphoblastic leukaemia) cells and the human melanoma SK-MEL-1 (ACC-303) and MEL-HO (ACC-62) cells were obtained from the German Collection of Microorganisms and Cell Cultures (Braunschweig, Germany). U-937/Bcl-2 cells were kindly provided by Dr. Jacqueline Bréard (INSERM U749, Faculté de Pharmacie Paris-Sud, Châtenay-Malabry, France). Cells were cultured in RPMI 1640 medium containing 10% (v/v) fetal bovine serum, 100 $\mu\text{g}/\text{mL}$ streptomycin and 100 U/mL penicillin, incubated at 37 °C in a humidified atmosphere containing 5% CO_2 as described [40]. Human peripheral blood mononuclear cells (PBMC) were isolated from blood anticoagulated with heparin of healthy donors by centrifugation with Ficoll-Paque Plus (GE Healthcare Bio-Sciences AB, Uppsala, Sweden). PBMC were also stimulated with phytohemagglutinine (2 $\mu\text{g}/\text{mL}$) for 48 h before the experimental treatment. Viability was always greater than 95% in all experiments as determined by the trypan blue exclusion method.

5.7. Cytotoxicity assays

The cytotoxicities of synthetic compounds were evaluated by colorimetric MTT [3-(4,5-dimethyl-2-thiazolyl)-2,5-diphenyl-2H-tetrazolium bromide] assays as described [41]. Compounds were dissolved in DMSO (dimethyl sulfoxide) and kept under dark conditions at 25 °C. Before each experiment, compounds were dissolved in culture media at 37 °C. The final concentration of DMSO did not exceed 0.3% (v/v). Cells (5,000 per well) were incubated with increasing concentrations of compounds for 72 h into a 96-well plate. Then, the supernatant was removed and MTT (0.5 mg/mL) was added and incubated at 37 °C for 4 h and the reaction products were solubilized with sodium dodecyl sulfate (10% w/v) in 0.05 M HCl overnight under dark conditions. Absorbance was measured at 570 nm using an ELISA reader (Bio-Rad) and the IC_{50}

values were determined graphically for each experiment by a nonlinear regression using the curve-fitting routine implemented within the software Prism 5.0 (GraphPad).

5.8. Soft agar colony formation assay

Cells (1,000) were grown in a layer of soft agar (0.3% w/v) mixed with RPMI 1640 cell culture medium that rested on another layer of soft agar (0.5% w/v), also mixed with RPMI 1640 medium in 6-well plates and incubated with the indicated concentrations of FMC or etoposide for twelve days. Then, cells were stained by adding 200 μ L of nitroblue tetrazolium chloride solution (1 mg/mL in PBS) per well and plates were incubated overnight at 37 °C.

5.9. Evaluation and quantification of apoptosis by fluorescent microscopy and flow cytometry

Fluorescence microscopy analysis was carried out as previously described. Briefly, following treatments the cells were washed with PBS, fixed in 3% paraformaldehyde, stained with 20 μ g/mL of bisbenzimidazole trihydrochloride (Hoechst 33258) and visualized with fluorescent microscopy (Zeiss-Axiovert). Flow cytometric analysis of propidium iodide-stained nuclei and of double staining annexin V-FITC and propidium iodide cells was performed using a BD FACSVerse™ cytometer (BD Biosciences, San Jose, CA, USA) as previously described [41].

5.10. Tubulin polymerization assay

In vitro tubulin polymerization assays were performed with reagents as described by the manufacturer (Cytoskeleton Inc., Denver, CO, USA). Briefly, increasing concentrations of FMC were incubated with purified bovine brain tubulin in a buffer containing 1 mM GTP and 10% glycerol at 37 °C, and the increase in absorbance was measured at 340 nm in a Beckman Coulter DTX880 microplate reader at 37 °C and recorded every 30 s for 50 min.

5.11. Immunocytochemistry

Cells were treated with 3 μ M FMC for 12 h and processed for immunofluorescence using a monoclonal antibody against α -tubulin. Briefly, after treatments cells were pelleted by

centrifugation at $500\times g$ for 10 min, washed with PBS and adhered by cyto centrifugation on microscope slides. Adherent cells were fixed for 10 min at room temperature with 3% paraformaldehyde, washed once with PBS for 5 min, then 0.1 M glycine for 5 min at room temperature, followed with PBS, permeabilized (0.25% Triton X-100), washed with PBS and blocked with 5% BSA and 5% normal goat serum in PBS containing 0.025% Triton X-100 for 1 h. After washing twice with PBS, cells were incubated with 1% BSA in PBS containing 0.025% Triton X-100 containing anti- α -tubulin monoclonal antibody (#2125, Cell Signaling Technology, 1:100 dilution) overnight at 4 °C. After washing with PBS, cells were incubated with Alexa Fluor 594-conjugated goat anti-rabbit antibody (Invitrogen, 1:1,000 dilution) in the dark for 90 minutes. Then, cells were rinsed with PBS and mounted with Vectashield mounting medium (Vector Laboratories, Burlingame, CA, USA) containing DAPI (4',6-diamidino-2-phenylindole, 1.5 $\mu\text{g}/\text{mL}$). Cellular microtubules images were obtained by using an inverted Nikon Eclipse 80i microscope with a 40x objective.

5.12. Assay of caspase activity

Caspase activity was determined in cell lysates using specific colorimetric substrates. Briefly, cells were treated with 3 μM for different time periods (6 h-24 h), harvested by centrifugation ($1000\times g$ for 5 min at 4 °C), washed with PBS, lysed with a buffer (50 mM HEPES, pH 7.4, 1 mM dithiothreitol, 0.1 mM EDTA, 0.1% Chaps), spun ($17,000\times g$ for 10 min at 4 °C) and the supernatants normalized by protein concentration were used to determine caspase activity. The net increase of absorbance at 405 nm after incubation at 37 °C was indicative of enzyme activity. The colorimetric substrates were DEVD-*p*NA (*N*-acetyl-Asp-Glu-Val-Asp-*p*-nitroaniline), IETD-*p*NA (*N*-acetyl-Ile-Glu-Thr-Asp-*p*-nitroaniline) and LEHD-*p*NA (*N*-acetyl-Leu-Glu-His-Asp-*p*-nitroaniline) for caspase-3/7, -8 and -9 activities, respectively.

5.13. Western blot analysis and subcellular fractionation

Whole cell lysates and cytosolic fractions were subjected to immunoblot analysis as previously described. For whole cell lysates, cell pellets were resuspended in lysis buffer [20 mM Tris-HCl

(pH 7.4), 137 mM NaCl, 20 mM sodium β -glycerophosphate, 10 mM sodium fluoride, 2 mM tetrasodium pyrophosphate, 2 mM sodium orthovanadate, 2 mM EDTA, 10% glycerol, 1% Triton X-100 plus the protease inhibitors phenylmethylsulfonyl fluoride (PMSF, 1 mM), aprotinin, leupeptin and pepstatin A (1 μ g/mL each)], homogenized by a sonifier (five cycles) and centrifuged at 11,000x g for 10 min at 4 °C. Equal amounts of proteins from supernatants were loaded on a sodium dodecyl sulfate-polyacrylamide gel (10% for MAPKs and 12.5% for caspases and Bcl-2 family proteins). Proteins were electrophoretically transferred to poly(vinylidene difluoride) membranes and detected by enhanced chemiluminescence. For subcellular fractionation, cells were washed twice with PBS and then resuspended in ice-cold buffer [20 mM HEPES (pH 7.5), 250 mM sucrose, 10 mM KCl, 1.5 mM MgCl₂, 1 mM EDTA, 1 mM EGTA and 1 mM dithiothreitol containing protease inhibitors (0.1 mM PMSF and 1 μ g/mL leupeptin, aprotinin and pepstatin A)]. After 15 min on ice, cells were lysed by pushing them several times through a 22-gauge needle, and the lysate was centrifuged at 1,000x g for 5 min at 4 °C. This pellet was used as a nuclear fraction. The supernatant fraction was centrifuged at 105,000x g for 45 min at 4 °C, and the resulting supernatant was used as the soluble cytosolic fraction.

5.14. Analysis of mitochondrial membrane potential $\Delta\Psi_m$ and intracellular reactive oxygen species (ROS) determination

The mitochondrial membrane potential and intracellular ROS production were determined by flow cytometry using the fluorochromes 5,5',6,6'-tetrachloro-1,1',3,3'-tetraethylbenzimidazolylcarbocyanine iodide (JC-1, 5 μ g/mL) and 2',7'-dichlorodihydrofluorescein diacetate (H₂-DCF-DA, 10 μ M), respectively. Flow cytometric analysis was performed using a BD FACSVerse™ cytometer (BD Biosciences, San Jose, CA, USA) and has been described in detail elsewhere [42].

5.14. Statistical methods

Statistical differences between means were tested using (i) Student's t-test (two samples) or (ii) one-way analysis of variance (ANOVA) (3 or more samples) with Tukey's test used for a posteriori pairwise comparisons of means. A significance level of $P < 0.05$ was used.

Funding: This research was funded by Agencia Canaria de Investigación, Innovación y Sociedad de la Información (grant number CEI2019/05) and in part by the Spanish Ministry of Science, Innovation and Universities and the European Regional Development Fund (PGC2018-094503-B-C21 and PGC2018-094503-B-C22).

Acknowledgments: E.S. was supported by the Fundación Instituto Canario de Investigación del Cáncer. E. S.-L. is recipient of a predoctoral fellowship of Consejería de Economía, Conocimiento y Empleo del Gobierno de Canarias in co-financing with Fondo Social Europeo (TESIS2020010081).

Conflict of interest

The authors declare that there is no conflict of interest.

References

- [1] K.D. Miller, M. Fidler-Benaoudia, T.H. Keegan, H.S. Hipp, A. Jemal, R.L. Siegel, Cancer statistics for adolescents and young adults, 2020. *CA Cancer J. Clin.* 70 (2020) 443-459, <https://doi.org/10.3322/caac.21637>.
- [2] H. Sung, J. Ferlay, R.L. Siegel, M. Laversanne, I. Soerjomataram, A. Jemal, F. Bray, Global Cancer Statistics 2020: GLOBOCAN Estimates of Incidence and Mortality Worldwide for 36 Cancers in 185 Countries. *CA Cancer J. Clin.* 71 (2021) 209-249, <https://doi.org/10.3322/caac.21660>.

- [3] K.D. Miller, L. Nogueira, A.B. Mariotto, J.H. Rowland, K.R. Yabroff, C.M. Alfano, A. Jemal, J.L. Kramer, R.L. Siegel, Cancer treatment and survivorship statistics, 2019. *CA Cancer J. Clin.* 69 (2019) 363-385, <https://doi.org/10.3322/caac.21565>.
- [4] S. Elmore, Apoptosis: a review of programmed cell death. *Toxicol. Pathol.* 35 (2007) 495-516, <https://doi.org/10.1080/01926230701320337>.
- [5] O. Julien, J.A. Wells, Caspases and their substrates. *Cell Death Differ.* 24 (2017) 1380-1389, <https://doi.org/10.1038/cdd.2017.44>.
- [6] B.A. Carneiro, W.S. El-Deiry, Targeting apoptosis in cancer therapy. *Nat. Rev. Clin. Oncol.* 17 (2020) 395-417, <https://doi.org/10.1038/s41571-020-0341-y>.
- [7] L. Galluzzi, I. Vitale, S.A. Aaronson, J.M. Abrams, D. Adam, P. Agostinis, E.S. Alnemri, L. Altucci et al., Molecular mechanisms of cell death: recommendations of the Nomenclature Committee on Cell Death 2018. *Cell Death Differ.* 25 (2018) 486-541, <https://doi.org/10.1038/s41418-017-0012-4>.
- [8] D.J. Newman, G.M. Cragg, Natural Products as Sources of New Drugs over the Nearly Four Decades from 01/1981 to 09/2019. *J. Nat. Prod.* 83 (2020) 770-803, <https://doi.org/10.1021/acs.jnatprod.9b01285>.
- [9] E.R. Sauter, Cancer prevention and treatment using combination therapy with natural compounds. *Expert Rev. Clin. Pharmacol.* 13 (2020) 265-285, <https://doi.org/10.1080/17512433.2020.1738218>.
- [10] D. Ravishankar, A.K. Rajora, F. Greco, H.M. Osborn, Flavonoids as prospective compounds for anti-cancer therapy. *Int. J. Biochem. Cell Biol.* 45 (2013) 2821-2831, <https://doi.org/10.1016/j.biocel.2013.10.004>.
- [11] D. Raffa, B. Maggio, M.V. Raimondi, F. Plescia, G. Daidone, Recent discoveries of anticancer flavonoids. *Eur. J. Med. Chem.* 142 (2017) 213-228, <https://doi.org/10.1016/j.ejmech.2017.07.034>.
- [12] C. Forni, M. Rossi, I. Borromeo, G. Feriotto, G. Platamone, C. Tabolacci, C. Mischiati, S. Beninati, Flavonoids: A Myth or a Reality for Cancer Therapy?. *Molecules* 26 (2021) 3583, <https://doi.org/10.3390/molecules26123583>.

- [13] S. Shukla, A.K. Sood, K. Goyal, A. Singh, V. Sharma, N. Guliya, S. Gulati, S. Kumar, Chalcone Scaffolds as Anticancer Drugs: A Review on Molecular Insight in Action of Mechanisms and Anticancer Properties. *Anticancer Agents Med. Chem.* 21 (2021) 1650-1670, <https://doi.org/10.2174/1871520620999201124212840>.
- [14] Y. Ouyang, J. Li, X. Chen, X. Fu, S. Sun, Q. Wu, Chalcone Derivatives: Role in Anticancer Therapy. *Biomolecules* 11 (2021) 894, <https://doi.org/10.3390/biom11060894>.
- [15] K.C. Nicolaou, J.A. Pfefferkorn, H.J. Mitchell, A.J. Roecker, S. Barluenga, G.-Q.Cao, R. L. Affleck, J.E. Lillig, Natural Product-like Combinatorial Libraries Based on Privileged Structures. 2. Construction of a 10 000-Membered Benzopyran Library by Directed Split-and-Pool Chemistry Using NanoKans and Optical Encoding. *J. Am. Chem. Soc.* 122 (2000) 9954-9967, <https://doi.org/10.1021/ja002034c>.
- [16] M.D. Delost, D.T. Smith, B.J. Anderson, J.T. Njardarson, From oxiranes to oligomers: architectures of U.S. FDA approved pharmaceuticals containing oxygen heterocycles. *J. Med. Chem.* 61 (2018) 10996–11020, <https://doi.org/10.1021/acs.jmedchem.8b00876>.
- [17] P.A. Wender, V.A. Verma, T.J. Paxton, T.H. Pillow, Function-oriented synthesis, step economy, and drug design. *Acc. Chem. Res.* 41 (2008) 40-9, <https://doi.org/10.1021/ar700155p>.
- [18] P. Harris, P. Ralph, Human leukemic models of myelomonocytic development: a review of the HL-60 and U937 cell lines, *J. Leukoc. Biol.* 37 (1985) 407-422, <https://doi.org/10.1002/jlb.37.4.407>.
- [19] W. Chanput, V. Peters, H. Wichers, THP-1 and U937 Cells, in: K. Verhoeckx, P. Cotter, I. López-Expósito, C. Kleiveland, T. Lea, A. Mackie, T. Requena, D. Swiatecka, H. Wichers (Eds.), *The Impact of Food Bioactives on Health: in vitro and ex vivo models*, Springer, 2015, pp. 147-159.
- [20] C. Zhuang, W. Zhang, C. Sheng, W. Zhang, C. Xing, Z. Miao, Chalcone: A Privileged Structure in Medicinal Chemistry. *Chem. Rev.* 117 (2017) 7762-7810, <https://doi.org/10.1021/acs.chemrev.7b00020>.
- [21] S. Zhuang, J.T. Demirs, I.E. Kochevar, p38 mitogen-activated protein kinase mediates bid cleavage, mitochondrial dysfunction, and caspase-3 activation during apoptosis induced by

singlet oxygen but not by hydrogen peroxide. *J. Biol. Chem.* 275 (2000) 275:25939-25948, <https://doi.org/10.1074/jbc.M001185200>.

[22] M. Watabe, H. Kakeya, H. Osada, Requirement of protein kinase (Krs/MST) activation for MT-21-induced apoptosis. *Oncogene* 18 (1999) 5211-5220, <https://doi.org/10.1038/sj.onc.1202901>.

[23] S.G. Shiah, S.E. Chuang, Y.P. Chau, S.C. Shen, M.L. Kuo, Activation of c-Jun NH₂-terminal kinase and subsequent CPP32/Yama during topoisomerase inhibitor beta-lapachone-induced apoptosis through an oxidation-dependent pathway. *Cancer Res.* 59 (1999) 391-398.

[24] Y.R. Chen, W. Wang, A.N. Kong, T.H. Tan, Molecular mechanisms of c-Jun N-terminal kinase-mediated apoptosis induced by anticarcinogenic isothiocyanates. *J. Biol. Chem.* 273 (1998) 1769-1775, <https://doi.org/10.1074/jbc.273.3.1769>.

[25] D. Cao, X. Han, G. Wang, Z. Yang, F. Peng, L. Ma, R. Zhang, H. Ye, M. Tang, W. Wu, K. Lei, J. Wen, J. Chen, J. Qiu, X. Liang, Y. Ran, Y. Sang, M. Xiang, A. Peng, L. Chen, Synthesis and biological evaluation of novel pyranochalcone derivatives as a new class of microtubule stabilizing agents. *Eur. J. Med. Chem.* 62 (2013) 579-589, <https://doi.org/10.1016/j.ejmech.2013.01.007>.

[26] S. Kraege, K. Stefan, S.C. Kçhler, M. Wiese, Optimization of acryloylphenylcarboxamides as inhibitors of ABCG2 and comparison with acryloylphenylcarboxylates. *ChemMedChem* 11 (2016) 2547-2558, <https://doi.org/10.1002/cmdc.201600455>.

[27] T. Walle, N. Ta, T. Kawamori, X. Wen, P.A. Tsuji, U.K. Walle, Cancer chemopreventive properties of orally bioavailable flavonoids--methylated versus unmethylated flavones. *Biochem. Pharmacol.* 73 (2007) 1288-1296, <https://doi.org/10.1016/j.bcp.2006.12.028>.

[28] T. Walle, Methoxylated flavones, a superior cancer chemopreventive flavonoid subclass?. *Semin. Cancer Biol.* 17 (2007) 354-362, <https://doi.org/10.1016/j.semcancer.2007.05.002>.

[29] A.A. Sy-Cordero, T.N. Graf, S.P. Runyon, M.C. Wani, D.J. Kroll, R. Agarwal, S.J. Brantley, M.F. Paine, S.J. Polyak, N.H. Oberlies, Enhanced bioactivity of silybin B methylation products. *Bioorg. Med. Chem.* 21 (2013) 742-747, <https://doi.org/10.1016/j.bmc.2012.11.035>.

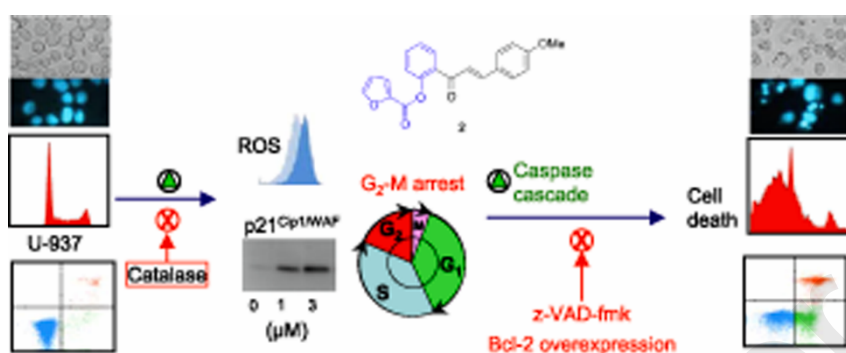
- [30] F. Grande, O.I. Parisi, R.A. Mordocco, C. Rocca, F. Puoci, L. Scrivano, A.M. Quintieri, P. Cantafio, S. Ferla, A. Brancale, C. Saturnino, M.C. Cerra, M.S. Sinicropi, T. Angelone, Quercetin derivatives as novel antihypertensive agents: Synthesis and physiological characterization. *Eur. J. Pharm. Sci.* 82 (2016) 161-170, <https://doi.org/10.1016/j.ejps.2015.11.021>.
- [31] M.K. Kim, K.S. Park, C. Lee, H.R. Park, H. Choo, Y. Chong, Enhanced stability and intracellular accumulation of quercetin by protection of the chemically or metabolically susceptible hydroxyl groups with a pivaloxymethyl (POM) promoiety. *J. Med. Chem.* 53 (2010) 8597-8607, <https://doi.org/10.1021/jm101252m>.
- [32] J.A. Beutler, E. Hamel, A.J. Vlietinck, A. Haemers, P. Rajan, J.N. Roitman, J.H. 2nd Cardellina, M.R. Boyd, Structure-activity requirements for flavone cytotoxicity and binding to tubulin. *J. Med. Chem.* 41 (1998) 2333-2338, <https://doi.org/10.1021/jm970842h>.
- [33] F. Estévez-Sarmiento, M. Said, I. Brouard, F. León, C. García, J. Quintana, F. Estévez, 3'-Hydroxy-3,4'-dimethoxyflavone blocks tubulin polymerization and is a potent apoptotic inducer in human SK-MEL-1 melanoma cells. *Bioorg. Med. Chem.* 25 (2017) 6060-6070, <https://doi.org/10.1016/j.bmc.2017.09.043>.
- [34] S. Rubio, J. Quintana, J.L.-Eiroa, J. Triana, F. Estévez, Betuletol 3-methyl ether induces G₂-M phase arrest and activates the sphingomyelin and MAPK pathways in human leukemia cells. *Mol. Carcinog.* 49 (2010) 32-43, <https://doi.org/10.1002/mc.20574>.
- [35] F. Torres, J. Quintana, F. Estévez, 5,7,3'-trihydroxy-3,4'-dimethoxyflavone-induced cell death in human leukemia cells is dependent on caspases and activates the MAPK pathway. *Mol. Carcinog.* 49 (2010) 464-475, <https://doi.org/10.1002/mc.20619>.
- [36] J.C. Goldstein, C. Muñoz-Pinedo, J.E. Ricci, S.R. Adams, A. Kelekar, M. Schuler, R.Y. Tsien, D.R. Green, Cytochrome c is released in a single step during apoptosis. *Cell Death Differ.* 12 (2005) 453-462, <https://doi.org/10.1038/sj.cdd.4401596>.
- [37] E. Bossy-Wetzel, D.D. Newmeyer, D.R. Green, Mitochondrial cytochrome c release in apoptosis occurs upstream of DEVD-specific caspase activation and independently of mitochondrial transmembrane depolarization. *EMBO J.* 17 (1998) 37-49, <https://doi.org/10.1093/emboj/17.1.37>.

- [38] J.N. Moloney, T.G. Cotter, ROS signalling in the biology of cancer. *Semin. Cell Dev. Biol.* 80 (2018) 50-64, <https://doi.org/10.1016/j.semedb.2017.05.023>.
- [39] Q. Peng, Z. Deng, H. Pan, L. Gu, O. Liu, Z. Tang, Mitogen-activated protein kinase signaling pathway in oral cancer. *Oncol. Lett.* 15 (2018) 1379-1388, <https://doi.org/10.3892/ol.2017.7491>.
- [40] E. Saavedra, H. Del Rosario, I. Brouard, J. Quintana, F. Estévez, 6'-Benzyloxy-4-bromo-2'-hydroxychalcone is cytotoxic against human leukaemia cells and induces caspase-8- and reactive oxygen species-dependent apoptosis. *Chem. Biol. Interact.* 298 (2019) 137-145, <https://doi.org/10.1016/j.cbi.2018.12.010>.
- [41] T. Mosmann, Rapid colorimetric assay for cellular growth and survival: application to proliferation and cytotoxicity assays. *J. Immunol. Methods* 65 (1983) 55-63, [https://doi.org/10.1016/0022-1759\(83\)90303-4](https://doi.org/10.1016/0022-1759(83)90303-4).
- [42] F. Estévez-Sarmiento, E. Hernández, I. Brouard, F. León, C. García, J. Quintana, F. Estévez, 3'-Hydroxy-3,4'-dimethoxyflavone-induced cell death in human leukaemia cells is dependent on caspases and reactive oxygen species and attenuated by the inhibition of JNK/SAPK. *Chem. Biol. Interact.* 288 (2018) 1-11, <https://doi.org/10.1016/j.cbi.2018.04.006>.

Declaration of interests

The authors declare that they have no known competing financial interests or personal relationships that could have appeared to influence the work reported in this paper.

The authors declare the following financial interests/personal relationships which may be considered as potential competing interests:



Highlights

New chalcones and flavonol derivatives were synthesized> A novel furoyloxychalcone showed strong cytotoxicity against human tumour cells> It induced cell cycle arrest in the G₂-M phase and apoptosis in human leukaemia cells > It showed less cytotoxicity against normal human peripheral blood mononuclear cells> Cell death was decreased by a pan-caspase inhibitor and catalase